

[2+2] DIMERIZATION OF CINNAMYLIDENEMALONIC ACID

A thesis presented to the faculty of the Graduate School of
Western Carolina University in partial fulfillment of the
requirements for the degree of Master of Science.

By

Shana Weathersby

Director: Dr. Brian Dinkelmeyer
Director of Graduate Program
Department of Chemistry and Physics

Committee Members: Dr. William Kwochka, Chemistry
Dr. Jack Summers, Chemistry

November 2010

Acknowledgements

I would like to thank Dr Dinkelmeyer for all his help along with my committee members, Dr. Kwochka and Dr. Summers. I would also like to thank Dr. Scott Huffman for his help in the FTIR/ATR study as well as the faculty and staff of Western Carolina University for giving me the opportunity to continue my studies. I would like to thank my family for all their support and my son Kaleb for being so understanding.

TABLE OF CONTENTS

ACKNOWLEDGEMENTS.....	ii
List of Tables.....	v
List of Figures.....	vi
List of Schemes.....	vii
ABSTRACT.....	viii
CHAPTER 1: INTRODUCTION.....	1
1.1 Topochemical Reactions.....	1
1.2 Topochemical Polymerizations.....	3
1.3 Supramolecular Chemistry.....	5
1.4 Project Design.....	6
CHAPTER 2: RESULTS AND DISCUSSION.....	10
2.1 Introduction.....	10
2.2 Host Synthesis.....	12
2.3 Guest Synthesis.....	12
CHAPTER 3: CRYSTAL STRUCTURES.....	16
3.1 Introduction.....	16
3.2 Crystal structure of N,N-bis(Pyridyl-4-ylmethyl)D-(S,S)-Tartaramide.....	17
3.3 Crystal structure of N,N-bis(Pyridyl-3-ylmethyl)D-(S,S)-Tartaramide.....	19
3.4 Crystal structure of N,N-bis(Pyridyl-2-ylmethyl)D-(S,S)-Tartaramide.....	20
3.4 Crystal Structure of Cinnamylidenemalonic acid.....	22

CHAPTER 4: PHOTOCHEMICAL STUDY OF CINNAMYLIDENEMALONIC ACID.....	26
4.1 Polymorphs of Cinnamylidenemalonic acid.....	26
CHAPTER 5: KINETICS STUDY OF THE [2+2] DIMERIZATION OF CINNAMYLIDENEMALONIC ACID.....	34
5.1 Introduction to Kinetics Study.....	34
5.2 Kinetics Study Results.....	41
5.3 Kinetics Study using FTIR/ATR.....	42
5.4 Kinetics Study using H ¹ NMR.....	49
CHAPTER 6: EXPERIMENTALS.....	52
REFERENCES.....	60
APPENDIX.....	62

LIST OF TABLES

Table

1.	List of compounds attempted in co-crystallization.....	11
2.	List of Attempted co-crystallizations.....	14
3.	Solubility Profile.....	15
4.	Table of equations used to calculate mole fractions.....	45
5.	Table of calculated mole fractions.....	46

LIST OF FIGURES

1. Crystals of Cinnamic acid and 2+2 cycloaddition reactions.....	1
2. Possible reactions dienes can undergo.....	3
3. Illustration of possible topochemical reactions of dienes.....	4
4. Space Groups.....	8
5. Project Design Image.....	9
6. Crystal Structure of N, N'-bis(pyridine-4-ylmethyl) D-(S,S)- Tartaramide.....	17
7. Crystal Structure of N,N'-bis(pyridine-4-ylmethyl) D-(S,S)-Tartaramide B-axis view.....	18
8. Crystal Structure of N,N'-bis(pyridine-3-ylmethyl) D-(S,S)-Tartaramide.....	19
9. Crystal Structure of N,N'-bis(pyridine-2-ylmethyl) D-(S,S)-Tartaramide.....	20
10. Crystal Structure of N,N'-bis(pyridine-2-ylmethyl) D-(S,S)-Tartaramide B-axis view.....	21
11. Crystal Structure of Cinnamylidenemalonic acid.....	22
12. Typical centrosymmetric dimer H-bonding pattern for carboxylic acids.....	24
13. The H-bonded tape and the 2-fold screw axis in cinnamylidenemalonic.....	25
14. Polymorph Powder Pattern.....	27
15. Images of polymorph 1.....	28
16. Images of polymorph 2.....	29
17. Images of polymorph 3.....	30
18. Cinnamylidenemalonic acid NMR's.....	31
19. Polymorphs 2+3 NMR's after sunlight.....	32
20. Packing parameters for the 2+2 cyclization.....	34
21. Polymorph head to tail stacking parameters.....	36
22. Possible reaction pathway one of cinnamylidenemalonic acid.....	37
23. Two possible reaction pathways of cinnamylidenemalonic acid.....	38
24. NMR representing a sample exposed to light.....	39
25. C ¹³ of predicted crystalline structure of cinnamylidenemalonic acid.....	40
26. Representation of the Infrared of polymorph 2 over a period of 177 min.....	43
27. Illustration of the monomer and dimer: $A_m = \epsilon_m b[\text{monomer}]$ and $A_d = \epsilon_d b[\text{dimer}]$..	44
28. Zero order reaction: mole fraction versus time.....	47
29. First order reaction Natural log of mole fraction versus time.....	48
30. Second order reaction inverse mole fraction versus time.....	48
31. NMR illustration of changes over time occurring in aromatic region.....	50

LIST OF SCHEMES

1. Pathway to Tartaramide and to Ester.....	12
2. Pathway to Cinnamaldehyde.....	13
3. Pathway to Cinnamylidenemalonic acid.....	14
4. Photochemical reaction of Cinnamylidenemalonic acid.....	41

[2+2] Topochemical Dimerization of Cinnamylidene Malonic Acid**Shana Weathersby****Western Carolina University****Advisor: Dr. Dinkelmeyer****Abstract:**

The original goal of the proposed research project was to crystallize a chiral host molecule with a diene-containing guest molecule to produce stereoselective molecules in a solid state reaction. These topochemical reactions occur within a crystalline matrix and impart the stereochemistry of the starting material to the product. Tartaric acid was used as a host because it was inexpensive and had a consistent mode of molecular packing and Muconic acid derivatives were synthesized and used as guest molecules. However, solubility problems prevented any co crystal reactions from taking place. Crystal structures were obtained for the host compounds. The focus of the rest of the project was then turned to a potential guest compound, cinnamylidenemalonic acid.

Cinnamylidenemalonic acid was found to crystallize in three different polymorphic structures each of which underwent photochemical reaction when irradiated with 257.3A of light. Products of photochemical reactions were characterized by proton NMR. Polymorph 1 gave a mixture of products, while polymorphs 2 and 3 formed the same [2+2] dimerization product. Infrared spectroscopy and proton NMR were used to study the solid state photochemistry of the compound in an attempt to find a suitable rate law.

CHAPTER 1 BACKGROUND

1.1 Topochemical Reactions

The first recognition of the feature of solid state organic reactions and its importance dates back to the 1960's -70's Schmidt coined the term "crystal engineering" in the context of photodimerisation.^{11, 12} The original idea behind crystal engineering was to design organic molecules that would adopt particular crystal structures within which topochemical reactions could take place, which would lead to regioselective and stereoselective medium.²

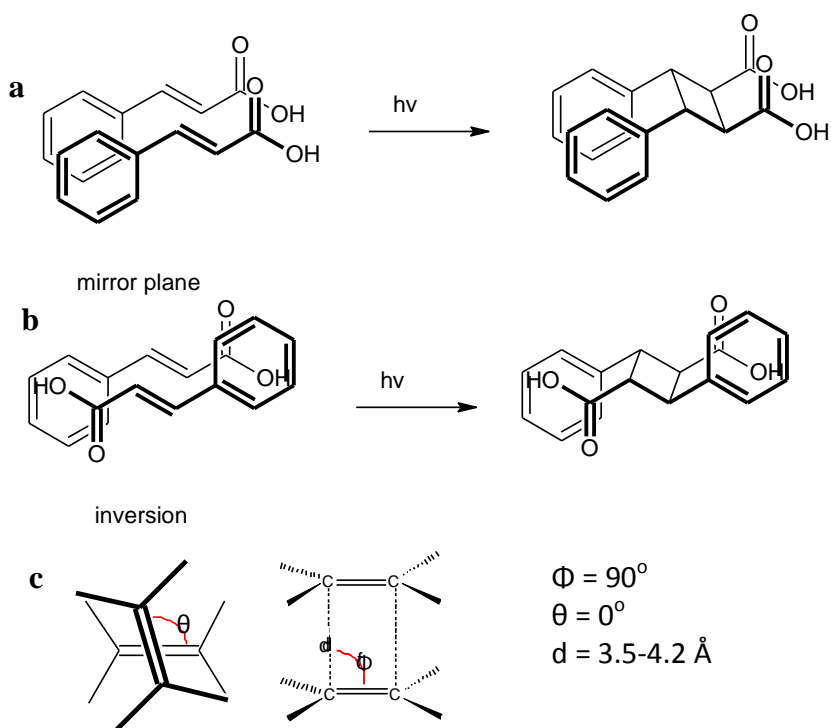


Figure : Crystals of cinnamic acid undergo 2+2 cycloaddition reactions. The regiochemistry and stereochemistry are determined by the crystal packing. a) Reactants are related by mirror plane which is retained in the product. b) Reactants are related by an inversion center which is retained in the product. c) Packing parameters necessary for the 2+2 reaction.

The first known example of this 2+2 cyclization reaction was with Cinnamic acid by Schmidt and Cohn¹⁵ when they found that the molecular packing in the starting material determined the outcome of these topochemical reactions. The crystal packing determines the relative orientation between the reacting species. The regiochemistry will be determined by the molecular packing since those atoms in close contact to the reactive atoms in neighboring molecules could undergo reaction. The stereochemistry was fixed by the molecular packing since the spatial orientation of the reacting cinnamic acid molecules was preserved in the final product.¹⁵ Reactant molecules that were related by mirror planes produced products that contained such and reactant molecules that were related by inversion centers produced products that contained inversion centers. When dealing with reactions in crystals, the packing of molecules has a great influence on the overall reactivity as well as regiochemistry and stereochemistry.

Cohen and Schmidt had found similar results in samples of other crystalline alkenes and were able to understand the packing parameters that were necessary for these reactions to occur. They were able to propose the topochemical postulate which states that "solid state reactions will occur with the least amount of motion."¹⁶ This is because of the very rigid environment that the reaction can occur in. Movement will displace the center of gravity and therefore hinder the reaction. The parameters that will allow for the 2+2 reactions to occur is when the reacting carbons are within 3.6-4.1 Angstroms and that they are parallel and not be offset.

It is important to know that even when all the parameters are in place, there is no guarantee that this reaction will occur. To be successful, any product that

forms will need to fit within the crystal lattice. If this doesn't happen, the crystal will be destroyed and the reaction will not proceed. These findings by Schmidt and Cohen have been found to apply to other solid state organic reactions.

1.2 Topochemical Polymerization

Topochemistry refers to reactions that occur within crystals and other materials such as monolayer where molecules have limited movement. Topochemical reactions are intended to yield structures that are highly controlled by the crystal lattice of the reactant.^{8,17} The focus is mainly on these reactions using conjugated dienes. There are two possible reactions that they can undergo; 2+2 and 1-4 topochemical polymerizations.

(Fig 2)

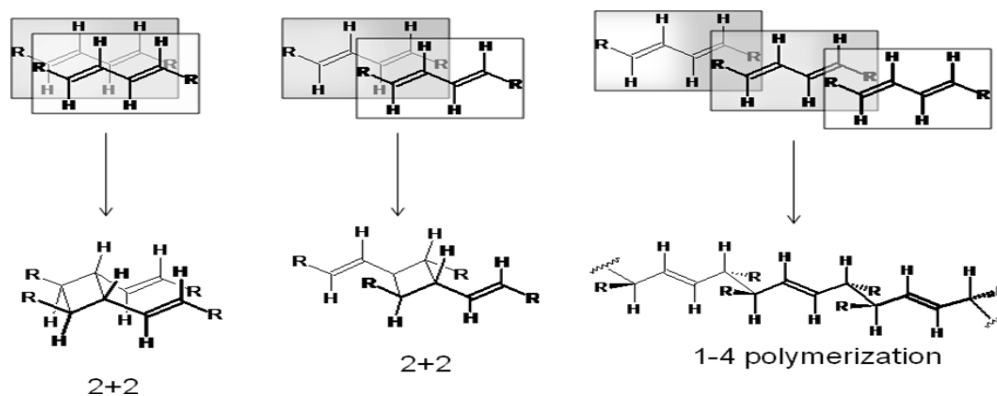


Figure 2: The figure above represents possible reactions dienes can undergo and it will depend on the spacing and how the molecule is lined up.

Topochemical polymerization is one of the most powerful methods for controlling the structure of both polymers. A topochemical polymerization process requires the favorable prearrangement of monomers in the crystals. There are very few polymerizations in the solid state that have been successful. All the included reactions are highly regulated under a crystal lattice control and polymers are obtained in crystalline form as reaction products. Controlling reactivity basically means controlling how monomers stack. The general approach for designing a topochemical polymerization involves matching the molecular repeat of an extended polymer with the periodic dimensions of a 1D network. This ensures that the polymer formed can fit within the crystal lattice.

The packing parameters for the 1-4 polymerization have been discussed by Matsumoto and Akikazu.^{1,2} These differ from the 2+2 reactions in that the similar carbon atoms should be between 4.5Å-5.0Å. At this distance, it is believed that p-orbital overlap is most likely to occur. If the dienes lie directly on top of one another they would not be properly aligned for polymerization. There needs to be a favorable tilt angle in order for the atoms to line up accordingly. Reacting monomers must be offset to allow C1 of one monomer to come in contact with C4 of a neighboring monomer. This angle of this offset has been defined as θ_1 and θ_2 . For the 1-4 polymerizations, dienes should stack so that θ_1 is approximately 45° and θ_2 is between 50°-85°. (Fig 3)

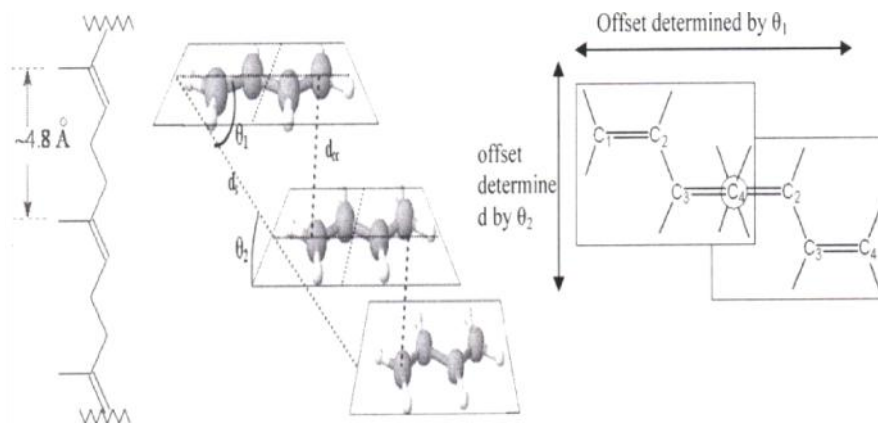


Figure 3: Illustration of possible topochemical reaction of dienes. Final product will depend on orientation of molecules within the crystal.

Predicting the reactivity and structure of polymer products are important in industry for the design of new organic solid materials. From the view point of polymer synthesis, crystal engineering is a very useful method in controlling the tacticity and molecular weight of polymers. There have been many attempts to control tacticity using free radical polymerization. The project was based on the research that was carried out using muconic and sorbic acid derivatives and created high molecular weight polymers^{1,2}.

1.3 Supramolecular Chemistry

As discussed, topochemical reactions are controlled by the packing mode molecules adopt in a crystal. In order to design and discover new topochemical reactions it is apparent to control how molecules pack. The intermolecular interactions that are utilized as elements of design for the arrangement and control of the molecules have been termed “synthons”.⁷ Synthons are used for the rational design of crystal and co-crystals

using molecular self assembly. (Fig 4)¹⁰ The figure below is a representation of synthons that can be used in to control how molecules arrange themselves within a crystal. By choosing the appropriate synthons an educated guess can be made with regards to the crystals structure. Strong hydrogen bonds are most commonly used for the controlled molecular packing to realize a rational design for the crystal structure of organic solids in the context of crystal engineering.

1.4 Project Design

The goal was to create a stereoselective solid state polymerization of diene containing molecules.^{1, 2,8,17} Previous researches of topochemical reactions was done using muconic esters and hexadienoic acid derivatives². In order to be successful, the reacting monomers will need to be arranged carefully within the crystal so that the reaction occurs with as little movement as possible. Usually, this will require that the reacting monomers be stacked with consistent distance and similar spacing. For polybutadienes, the distance is approximately 4.5-5.0 Å.⁴ Polymers containing amide groups have been shown to have the stacking distance between 4.8-5.1 Å.²⁴

When it comes to the stereochemistry of topochemical polymerizations, it's the monomers stacking that will determine the outcome. The symmetry relating reactant molecules is retained by the product which would suggest that the stereoselectivity for reactions that occur in crystals would be 100%. However, most topochemical reactions produce racemic mixtures because of crystallographic symmetry. Racemic products may be avoided by performing the reactions in a chiral space group. These symmetry

operations are not present in chiral space groups. Molecules in chiral space groups are related by only translational and rotational axis. The concept is illustrated in Figure 5 as it pertains to 1-4 topochemical polymerizations. In figure 4, the molecules are in achiral space groups and have both inversion centers and glide planes. However, even if a chiral polymer product is formed, a racemate will be produced if the space group of the crystal is achiral and occurs since adjacent polymer chains will be related by inversion centers, mirror planes or glide planes. Neighboring polymers produced in these crystals are also related by these symmetry operations and are enantiomers producing a 50/50 mix of each polymer.

Molecules in chiral space groups are related only by translation and screw axis operations. Reactions in chiral crystals should produce only one stereoisomer. They contain no inversion centers, glide planes or mirror planes and neighboring polymers produced in these crystals are related only by translational operations, so there should be 100% enantioselectivity.

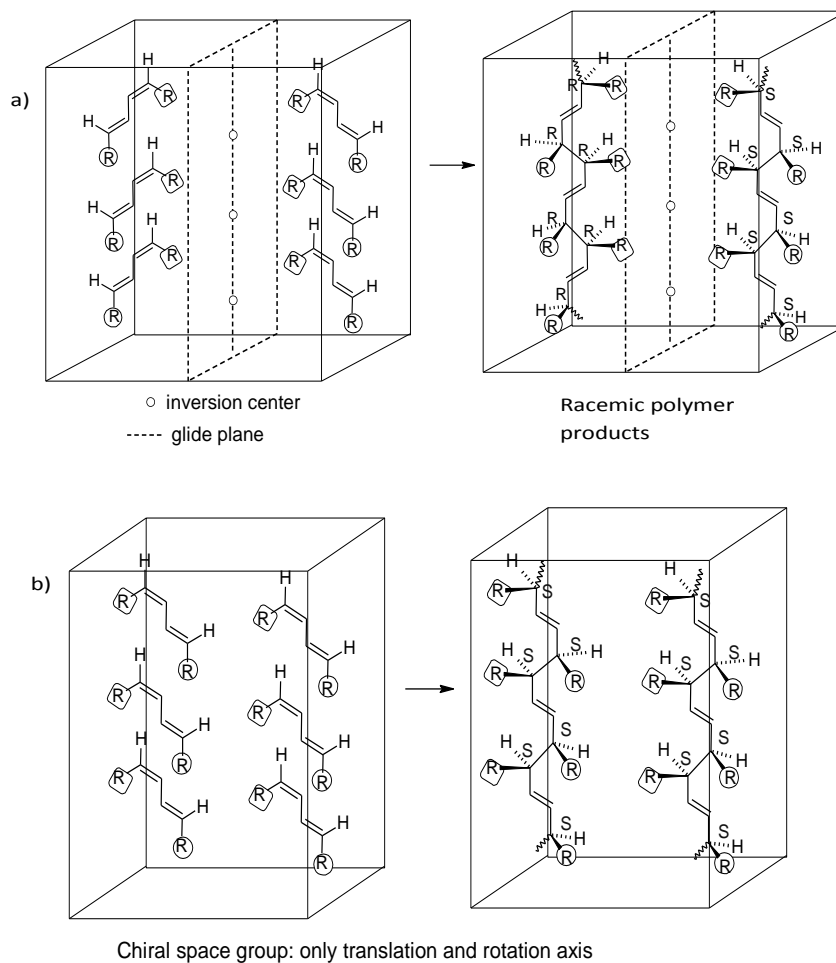


Figure 4: a) cis-trans diene within an achiral crystal system and its polymer products. Adjacent polymers within the crystal are enantiomers. b) cis-trans diene in a chiral crystal and its polymer products. Only one stereochemistry should form.

The project design was based using chiral host molecules containing amide functional groups. This design should space diene monomers at the required 4.8-5Å spacing and provide a chiral reaction environment. Tartaric acid has been shown to organize itself in a lattice with the required spacing which is another reason we chose to use it in this study. (Fig 5)⁵

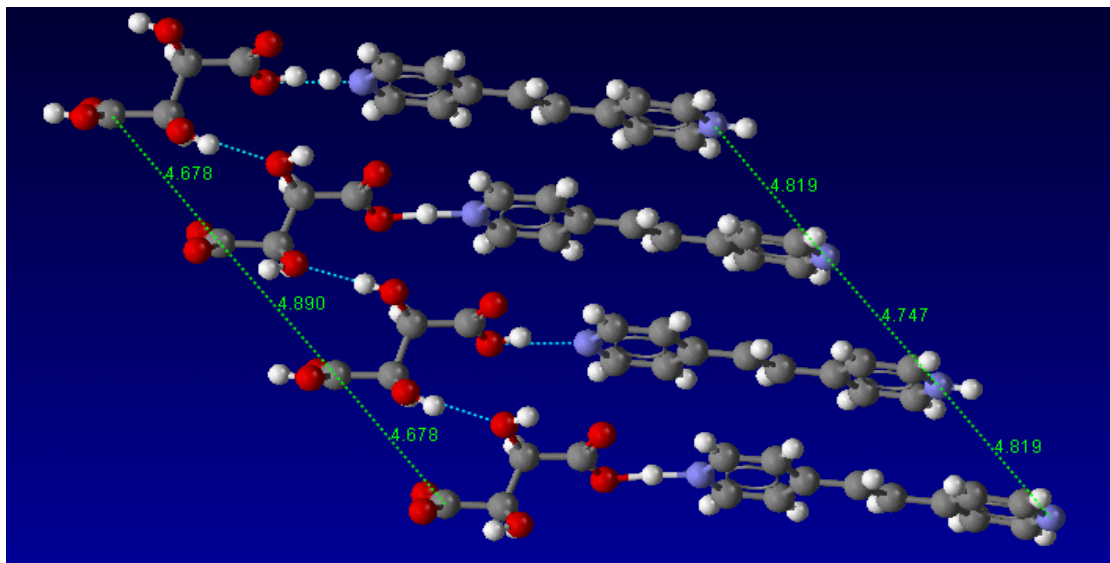


Figure 5: Structure of Tartaric acid and Dipyritylstilbene. The figure illustrates that Tartaric acid forms the needed polymer at the appropriate distance. (Cambridge Structural Database)

In pursuing this goal a number of tartamides host molecules and diene guest molecules were synthesized. Attempts at forming co-crystals containing both host and guest molecules was attempted. However, solubility problems prevented any co crystal reactions from taking place. Crystal structures were obtained for the host compounds. The focus of the project was then turned to a potential guest compound, cinnamylidenemalonic acid, which underwent 2+2 photodimerization.

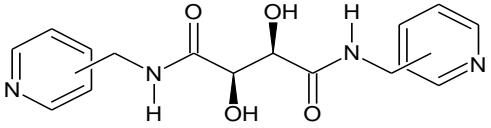
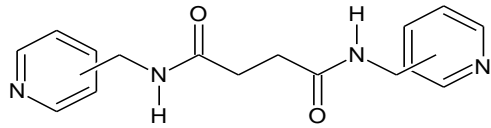
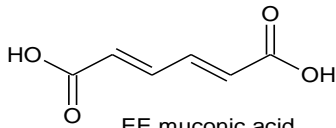
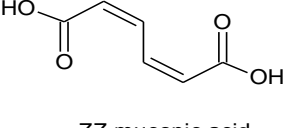
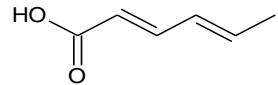
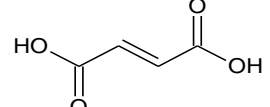
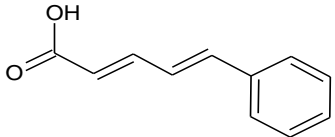
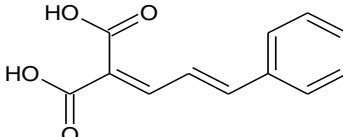
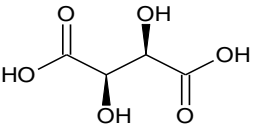
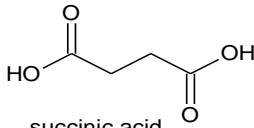
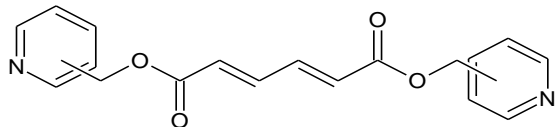
CHAPTER 2: RESULTS AND DISCUSSION

2.1 INTRODUCTION

The goal of the project was to co-crystallize the host molecules with the guest molecules hoping that the position of the functional groups would guide the molecules into an orientation that would allow for polymerization. The co-crystal approach would employ host molecules whose function would be to organize monomer/guest molecules for a solid-state reaction. The host guest strategy would allow for the generation of families of structurally related co-crystals and allow a systematic study of structural parameters important for reactivity. Factors such as the number and position of hydrogen bonding functional groups and the mobility within the crystal can and influence the solid-state reactivity.

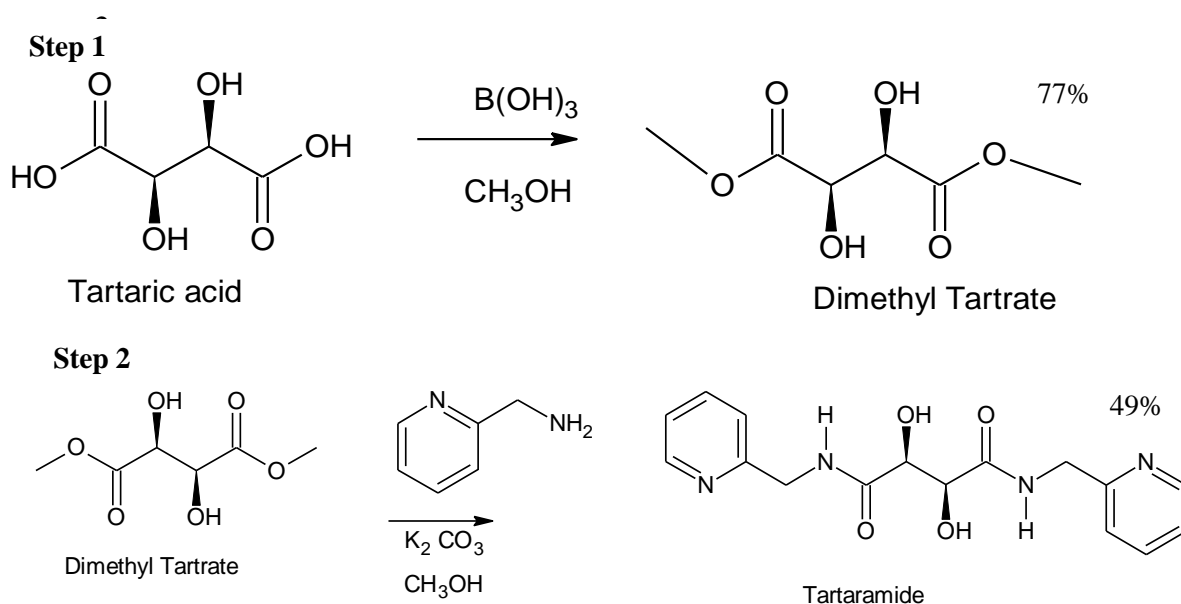
The project required that a number of host and guest molecules be synthesized. The host molecules (Tartaramides) were classified as H-bond acceptors/ Lewis bases and by the ability to hydrogen bond with the guest molecules. The guest molecules (Muconic acid and derivatives) were classified as H-bond donors/ Lewis Acids. These molecules had the capabilities to interact with each other due to the position of their functional groups. (Table 1)

Table 1: list of compounds that were attempted in the project

HOST MOLECULES	GUEST MOLECULES
<p><u>pyridyl hosts</u></p>  <p>pyridyl tartaramides</p>  <p>pyridyl succinamides</p>	<p><u>acid guests</u></p>  <p>EE muconic acid</p>  <p>ZZ muconic acid</p>  <p>hexadienoic acid</p>  <p>fumaric acid</p>  <p>5-phenyl 2,3-dienoic acid</p>  <p>cinnamylidene malonic acid</p>
<p><u>acid hosts</u></p>  <p>tartaric acid</p>  <p>succinic acid</p>	<p><u>pyridyl guests</u></p>  <p>pyridyl mucanoates</p>

2.2 Host Synthesis

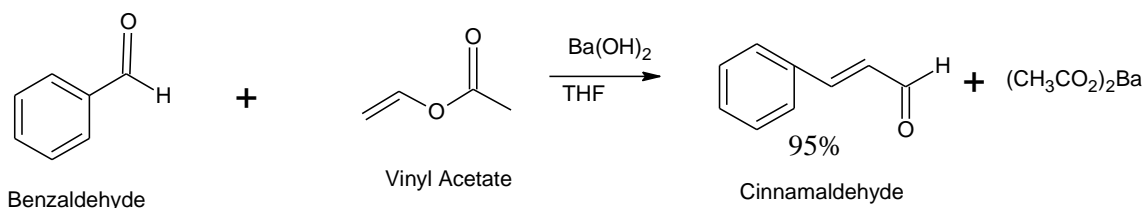
The Tartaramides were produced using a two step synthesis. The first step was the production of the Dimethyl Tartrate Ester.¹⁸ This was a simple esterification reaction using boric acid as a catalyst. The reaction produced a tetrahedral intermediate followed by the elimination of methanol. (Scheme 1) The Dimethyl Tartrate ester was then reacted with either 2, 3, or 4 amino-methyl pyridine by using a nucleophilic substitution and yielded the N, N'-bis (pyridine-2, 3, or 4-ylmethyl) D-(S, S)-Tartaramide¹⁸(Scheme 1)



Scheme 1: Step 1 Pathway to Tartrate. Step 2 Pathway to Tartaramide.

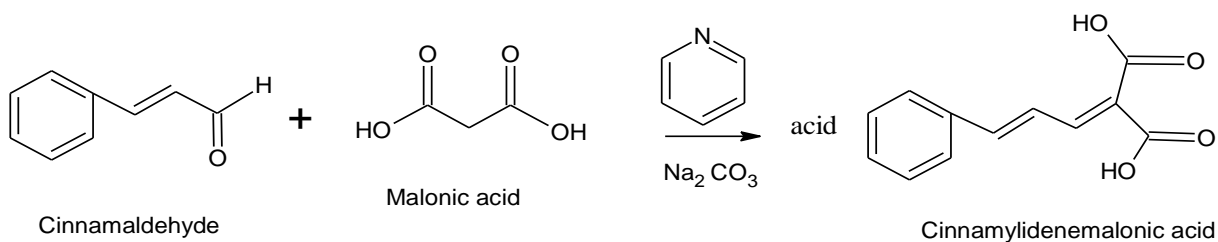
2.3 Guest Synthesis

A number of guest molecules were needed for the project. The trans-trans Muconic acid and cis-cis Muconic acid and Fumaric acid were readily available for the project, while others had to be synthesized. Cinnamaldehyde was produced from an Aldol reaction and prepared from Benzaldehyde and Vinyl Acetate.²⁰(Scheme 2)



Scheme 2 Reaction pathway to Cinnamaldehyde

The Cinnamylidene Malonic acid was the prepared from Cinnamaldehyde, malonic acid, and Pyridine.²¹(Scheme 3)



Scheme 3: Synthesis of cinnamylidenemalonic acid

2.4 Co-crystallizations

Several attempts were made at growing co-crystals using the host and guest molecules in Table 1. A significant amount of time and effort was spent on this endeavor with little success. In general, it is more difficult to grow crystals of chiral molecules than achiral molecules. Table 2 lists the host-guest co-crystals attempted. In each

attempt, host and guest molecules were dissolved in a solvent with a 1:1 or 1:2 mole ratio depending on the number of H-bond donor and acceptor groups they had. Various solvents were tried. During the trials, solubility was a problem because either the host crystallized or the guest crystallized in solution. It was difficult both the host and the guest together. . The ideal solvent for growing co-crystal is one in which both component molecules have equal solubility. If one component has a greater solubility than the other it tends to stay in solution while the less soluble component crystallizes by itself. The following is a synopsis of the different strategies that were attempted.

COMPOUNDS	SOLVENTS	SPECTRA	COXTAL	METHOD
3-L-PYR-TART/EE M.A	METHANOL	N/A	N/A	SLOW EVAPORATION
2-L-PYR-TART/ZZ M.A	METHANOL	N/A	N/A	SLOW EVAPORATION
3-L-PYR-TART/2,4 HEXA	ETHANOL	N/A	N/A	SLOW EVAPORATION
3-PYR-TART/TT M.A	ETHANOL	N/A	N/A	SLOW EVAPORATION
4-PYR-TART/CC M.A	ETHANOL	N/A	N/A	SLOW EVAPORATION
3-PYR-TART/2,4 HEXA	METHANOL	FTIR/ATR	NO	SLOW EVAPORATION
4-L-PYR-TART/2,4 HEXA	METHANOL	FTIR/ATR	NO	SLOW EVAPORATION
4-L-PYR-TART/TTM.A	ETHANOL	FTIR/ATR; HNMR	NO	SLOW EVAPORATION
4-L-PYR-TART/2,4 HEXA	ETHANOL	IR HNMR	NO	SLOW EVAPORATION
3-L-PYR-TART/2,4 HEXA	METHANOL	HNMR IR	NO	SLOW EVAPORATION
4-L-PYR-TART/TT MA	METHANOL	FTIR/ATR; HNMR	NO	SLOW EVAPORATION
4-L-PYR-TART/TT MA	ETHANOL	HNMR IR	NO	SLOW EVAPORATION
3-L-PYR-TART/TT MA	METHANOL	FTIR/ATR	NO	SLOW EVAPORATION
3-L-PYR-TART/TT MA	METHANOL	FTIR/ATR	NO	SLOW EVAPORATION
3-L-PYR-TART/TT MA	methanol	FTIR/ATR; HNMR	N/A	SLOW EVAPORATION
3-L-PYR-TART/TT MA	METHANOL/ETHYL ACETATE	N/A	N/A	SLOW EVAPORATION
3-L-PYR-TART/TT MA	METHANOL	N/A	N/A	SLOW DIFFUSION
2-L-PYR-TART/2,4 HEXA	DICHLOROMETHANE	N/A	NO	SLOW EVAPORATION
3-L--PYR-TART/TT M.A	ACETONITRILE	N/A	NO	SLOW EVAPORATION
2-L-PYR-TART/FUMARIC ACID	DICHLORMETHANE/ETOH	N/A	NO	SLOW EVAPORATION
2-L-PYR-TART/FUMARIC ACID	METHANOL	N/A	NO	SLOW EVAPORATION
2-L-PYR-TART/FUMARIC ACID	DICHLORMETHANE	N/A	NO	SLOW EVAPORATION
2-L-PYR-TART/FUMARIC ACID	ACETONITRILE	H-NMR,IR,C ¹³	NO	SLOW EVAPORATION
2-L-PYR-TART/FUMARIC ACID	ACETONE	H NMR IR C13	NO	SLOW EVAPORATION
3-L-PYR-TART/FUMARIC ACID	WATER	N/A	NO	SLOW EVAPORATION
2-L-PYR-TART/FUMARIC ACID	ACETONE	FTIR/ATR	NO	SLOW EVAPORATION
3-L-PYR-TART/FUMARIC ACID	ACETONITRILE	N/A	NO	SLOW EVAPORATION
3-L-PYR-TART/FUMARIC ACID	ETHYL ACETATE	N/A	NO	SLOW EVAPORATION
3-L-PYR-TART/FUMARIC ACID	METHANOL	N/A	NO	SLOW EVAPORATION
4-L-PYR-TART/FUMARIC ACID	ETHANOL	N/A	NO	SLOW EVAPORATION
4-L-PYR-TART/FUMARIC ACID	METHANOL	N/A	NO	SLOW EVAPORATION
4-L-PYR-TART/FUMARIC ACID	ACETONITRILE/WATER	N/A	NO	SLOW EVAPORATION
2-L-PYR-TART/FUMARIC ACID	ACETONE	N/A	NO	SLOW EVAPORATION
2-L-PYR-TART/CC M.A	ACETONITRILE/WATER	HNMR;FTIR/ATR	NO	SLOW EVAPORATION
2-L-PYR-TART/SUCCINIC ACID	ETHYL ACETATE	N/A	NO	SLOW EVAPORATION
2-L-PYR-TART/TT M.A	DICHLOROMETHANE	N/A	NO	SLOW EVAPORATION
4-L-PYR-TART/FUMARIC ACID	ACETONITRILE/WATER	N/A	NO	SLOW EVAPORATION
4-PYR-TART/SUCCINIC ACID	ACETONITRILE/WATER	IR	NO	SLOW EVAPORATION
3-PYR-TART/FUMARIC ACID	METHANOL	FTIR/ATR; HNMR;C ¹³	YES	SLOW EVAPORATION

Table 2: List of Attempted co-crystals

After initial attempts to grow co-crystals by slow evaporation failed the experiments were repeated using siled glassware. Silation of glassware creates a hydrophobic surface on the glass and removes nucleation sites on the glass where crystal growth may occur. This forces crystal nucleation and growth to occur in the solvent and not on the sides of the glassware. Repeating the crystallizations in siled glassware did not yield any product.

A solubility profile was created for all of molecules that were studied to aid in finding the right solvent. (Table 3) The goal was to find host and guest molecules that had similar solubility in a given solvent and use this information to find host/guest combinations that would likely form co-crystals in that particular solvent. The solubility's were determined by making saturated solutions of each molecule in Ethanol, Methanol, Ethyl Acetate, Acetonitrile, Acetone, Dichloromethane and Water. Carefully measured volumes (1.0 or 5.0 ml) of these samples were then evaporated to dryness and the mass of the residue determine. Several attempts were made to co-crystallize the host and guest compounds using the appropriately determined solvent from the solubility profile.

Table 3: Solubility Profile. S = very soluble. N.A. = not measured. Numerical values have units of grams solute/ml solvent

HOSTS	ethanol	methanol	Ethyl acetate	acetonitrile	acetone	dichloro methane	water
2-L-PYRIDYL-TARTARAMIDE	S	S	0.0202	0.0162	0.0026	0.0551	0.7312
3-L-PYRIDYL-TARTARAMIDE	S	S	NA	0.0105	0.0044	0.024	NA
4-L-PYRIDYL-TARTARAMIDE	S	S	0.0177	0.0078	0.0039	0.0025	NA
GUESTS							
EE-MUCONIC ACID	0.0085	0.0215	0.0057	0.0057	0.0142	0.0487	0.1127
ZZ-MUCONIC ACID	0.0177	0.0304	0.0133	0.0133	0.0172	0.0008	0.0059
2,4-HEXDIENOIC ACID	0.1667	0.1183	0.0573	0.0573	0.1008	0.0983	0.022

CHAPTER 3: CRYSTAL STRUCTURES

3.1 Introduction

Although unsuccessful in co-crystallizing the hosts and guests molecules, there was success in crystallizing the Pyridyl Tartaramides and Cinnamylidene Malonic acid as well as obtaining the crystal structures for each.

In describing the crystal structures of organic molecules, it is customary to provide information on the following: quality of the data obtained (R factor), the space group, the number of molecules in the unit cell (Z), and the unit cell parameters. The intermolecular forces that are considered responsible for controlling the packing arrangement of the molecules are also described.

Typically, hydrogen bonds are described first since they are assumed to play the largest role in the determination of molecular stacking. They are then compared to crystal structures in the literature and the Cambridge Structural Database to interpret any differences in interaction. Since functional groups have a limited number of ways in which they can form hydrogen bonds and still fit within a crystal lattice, new modes of interaction may be discovered for future designs of crystalline solids.

Next, the topologies of hydrogen bonded networks are studied. These include discrete closed loops, 1-D tapes or stacks, 2-D layers or tapes and 3-D networks.²⁴ Patterns formed by the intermolecular interactions are then related to the unit cell axis and symmetry elements of the space group. It's understood that hydrogen bonded networks that lie along unit cell axis or are on or around symmetry elements are useful design elements and may play an important role in causing the observed packing arrangements.

3.2: Crystal Structure of N, N'-bis(pyridine-4-ylmethyl) D-(S,S)-Tartaramide

The crystal (Fig 6) has the necessary packing parameters that are needed for 1,4-polymerization. The distance between similar atoms is about 5.1 Å and Matsumoto discovered that for polymerization to occur, the distance between reacting atoms on adjacent monomers should be within 4.8 and 5.2 Å².

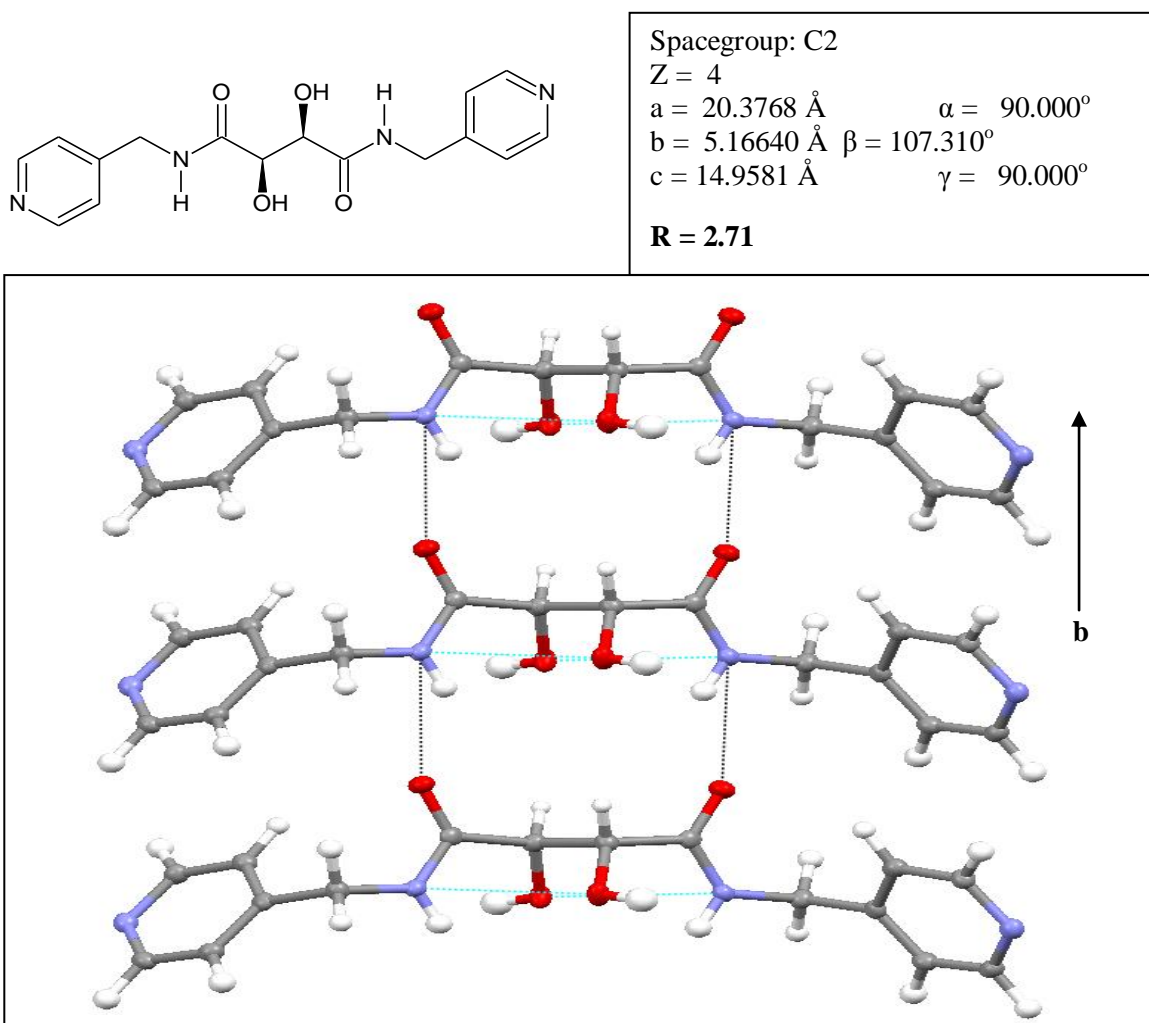


Figure 6: N,N'-bis(pyridine-4-ylmethyl) D-(S,S)-Tartaramide. This is a view looking down the C axis.

When molecules stack parallel to the B-axis, they are related by translation

Since it is also chiral, it must pack in a space group that is also chiral. The dipoles would be in the same direction and would, in turn, cancel each other out. In an achiral molecule, the directionality of the dipoles would alternate meaning that an inversion center or glide plane would be required. This is not seen in a chiral space group.

The molecule can form infinite 1-D hydrogen bonds tapes between the nitrogen atom on the pyridyl ring and the carboxylic acid oxygen of the neighboring monomer²⁴ (Fig 7). The view from the figure above is a view down the B-axis observing these hydrogen bonding stacks.

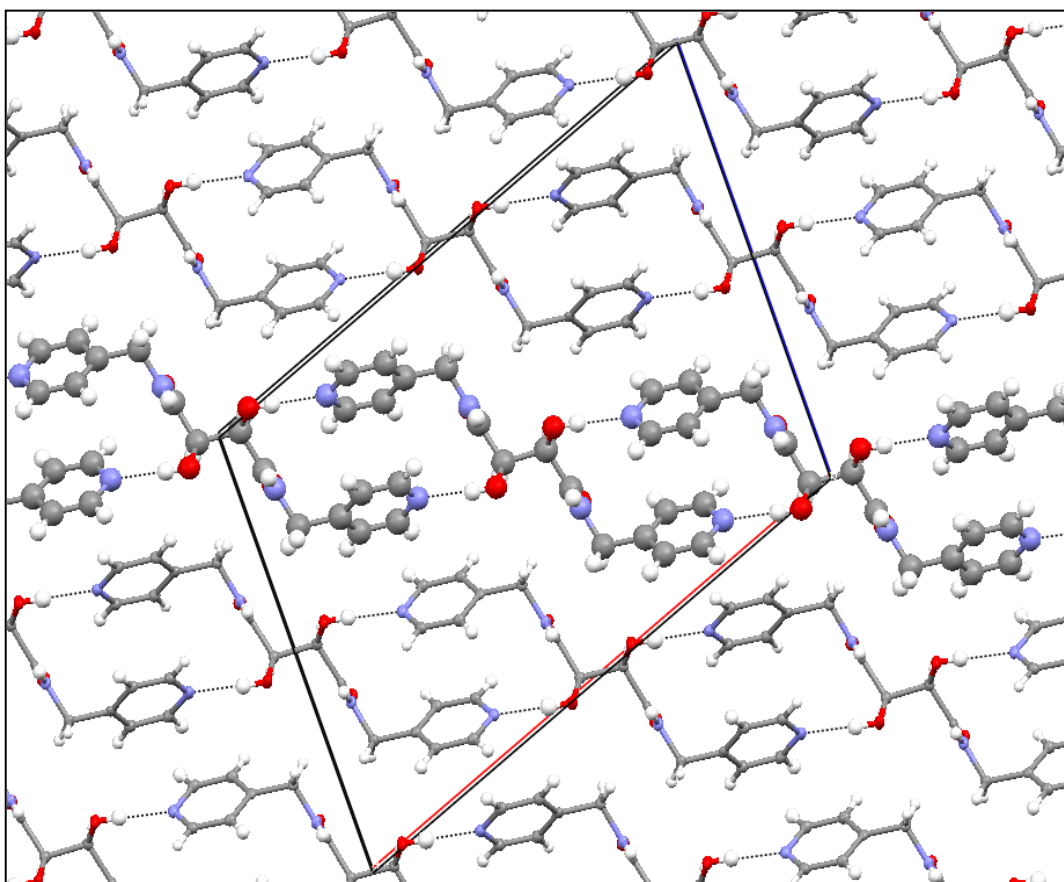


Figure 7: N,N'-bis(pyridine-4-ylmethyl) D-(S,S)-Tartaramide. This is a view looking down the B-axis and observing the Hydrogen bonding stacks.

3.3: Crystal Structure of N,N'-bis(pyridine-3-ylmethyl) D-(S,S)-Tartaramide

The N,N-bis(pyridine-3-ylmethyl) D-(S,S)-Tartaramide (Fig 8) is also a chiral molecule and would follow the same requirements as the previous structure. The crystal is polar and the dipoles cancel each other out. The reacting atoms of the adjacent monomers are approximately 5.0 angstroms and are within the parameters that were discussed by Matsumoto. With the molecule being chiral, would crystallize in a chiral space group and there is no inversion center or glide plane in this molecule.

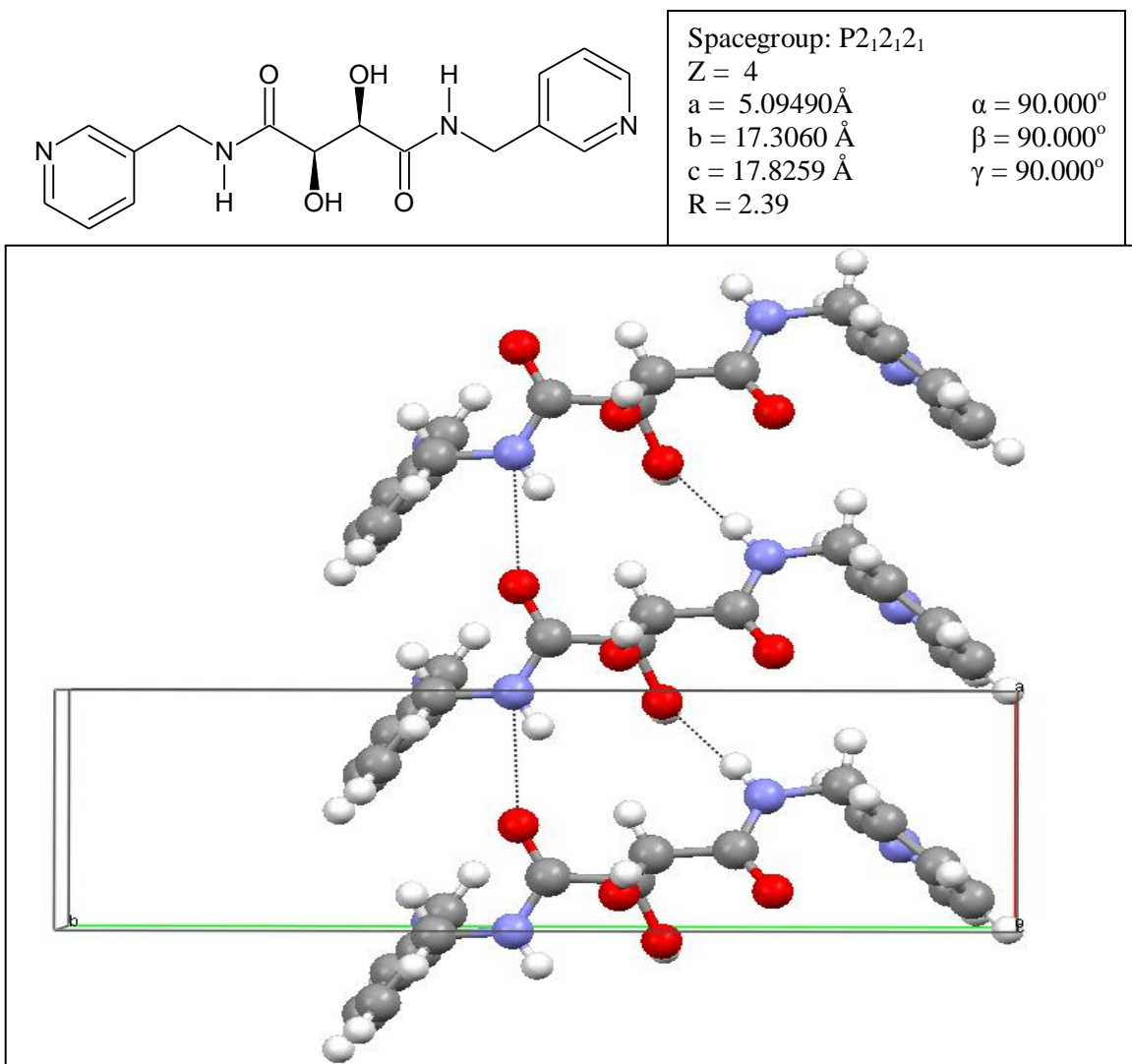


Figure 8: N,N'-bis(pyridine-3-ylmethyl) D-(S,S)-Tartaramide. View looking down the C axis. In this structure, notice that only one amide group forms the predicted N-H--O=C 1-D network.

3.4: Crystal Structure of N,N'-bis(pyridine-2-ylmethyl) D-(S,S)-Tartaramide

In this structure, the nitrogen atoms on the chain as well as the ring form an infinite bonding network²⁴ (Fig 9). The nitrogen's on the ring are hydrogen bonded to the hydroxyl hydrogen's and form a 1-D tape²⁴.

The spacing in the conformation of the N,N'-bis(pyridine-2-ylmethyl) D-(S,S)-Tartaramide makes it a potentially useful molecule for the project because based on the crystal structure, the distance between the dienes is 4.9 Å (Fig 9).

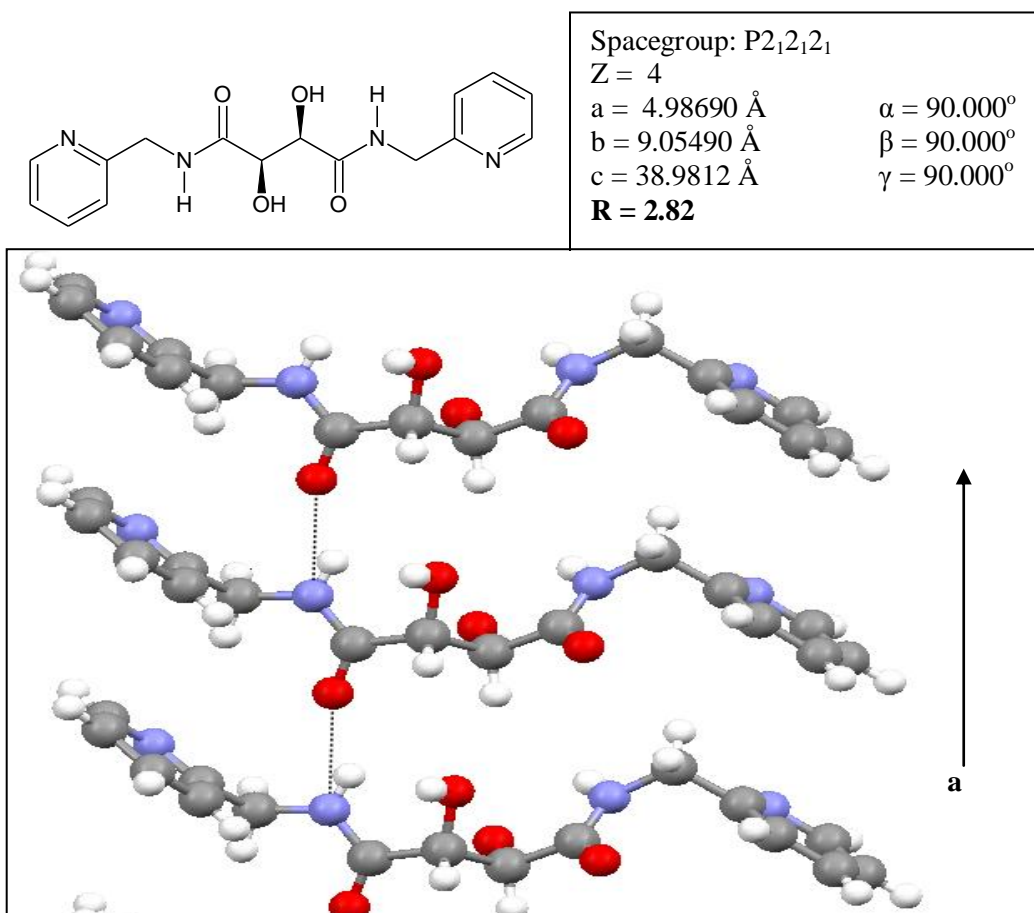


Figure 9: N,N'-bis(pyridine-2-ylmethyl) D-(S,S)-Tartaramide view down the b-axis. One N-H...O=C hydrogen network and is parallel to the a-axis. The other amide hydrogen network is along the b-axis.

The distance between the chains in the previous conformation is now approximately 5 Å (Fig 11). The intermolecular hydrogen bonding network that formed between the carboxylic acid on one chain and the hydrogen's related to the $-\text{CH}_2$ as well as the hydroxyl hydrogen's is known as a 3-centered network²⁴.

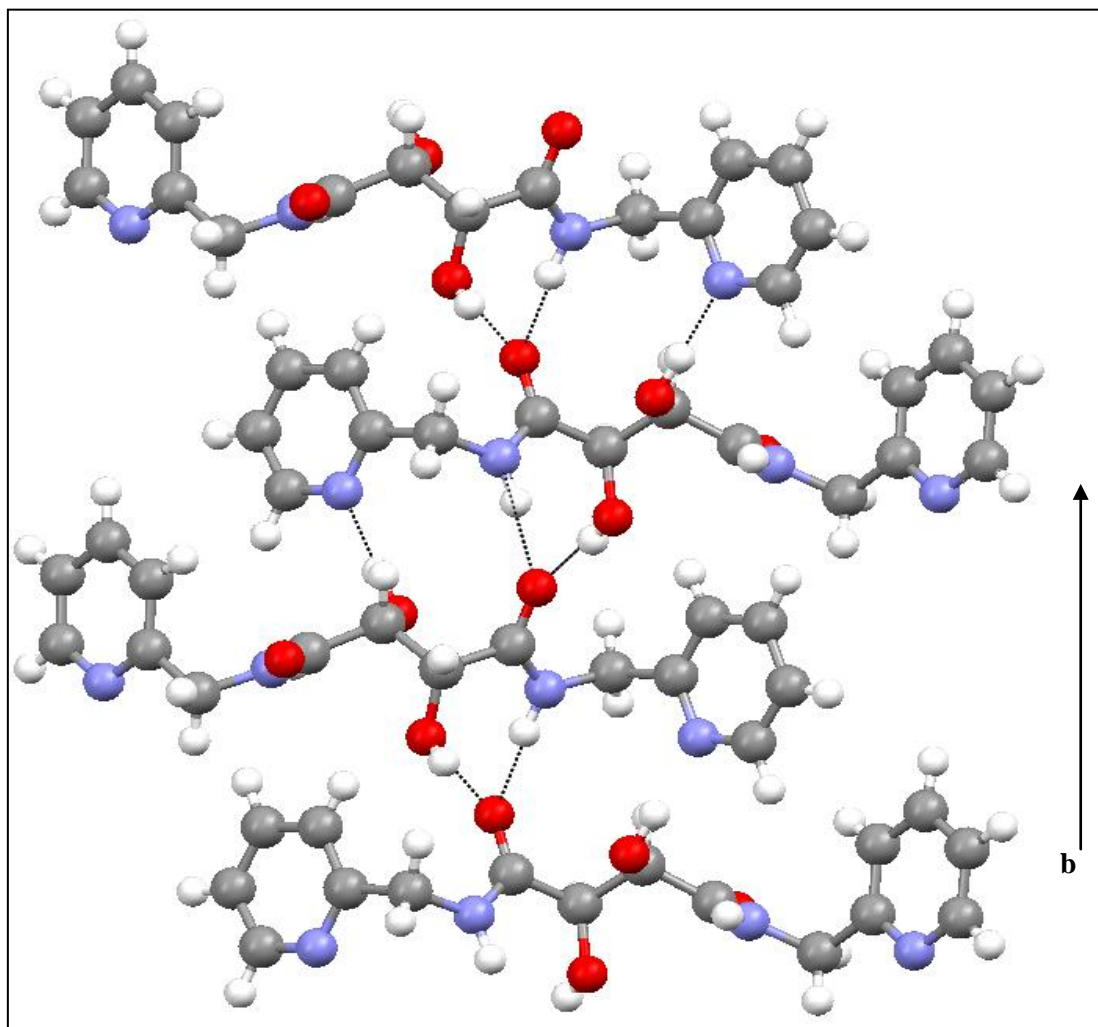
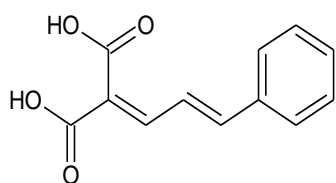


Figure 10: N,N'-bis(pyridine-2-ylmethyl) D-(S,S)-Tartaramide. In this view, the N-C=O---H-O-H network along the b-axis is clearly shown.

3.5: Crystal Structure of Cinnamylidenemalonic acid

Cinnamylidenemalonic acid is an achiral molecule and would crystallize in an achiral space group (Fig 11). In an achiral molecule, the directionality of the dipoles would alternate. This means that an inversion center or glide plane would be required which is what is seen here.



Spacegroup: $P2_1/c$

$Z = 4$

$a = 6.9763 \text{ \AA}$

$b = 10.4935 \text{ \AA}$

$c = 13.8570 \text{ \AA}$

$R = 5.73$

$\alpha = 90.000^\circ$

$\beta = 96.9330^\circ$

$\gamma = 90.000^\circ$

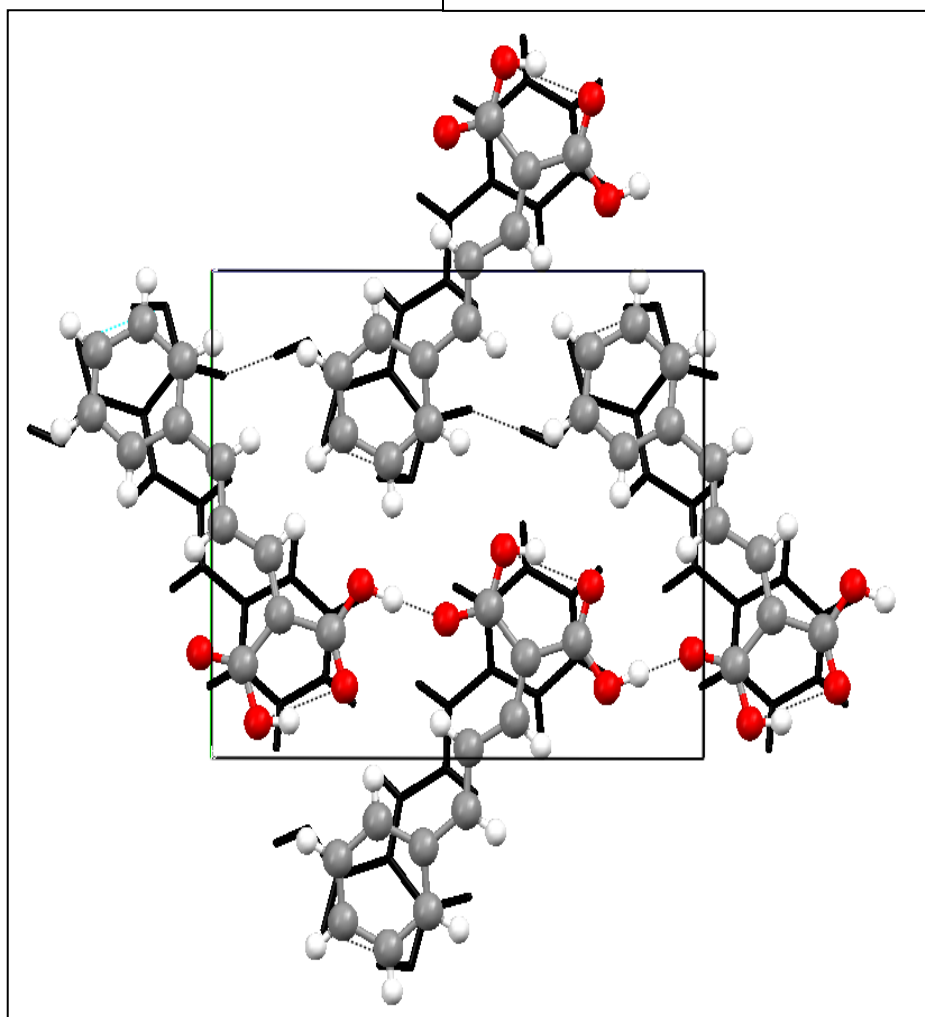


Figure 11: The crystal structure of Cinnamylidenemalonic acid viewed down the a-axis. Molecules are stacked in a head-to-tail arrangement along the a-axis.

The carboxylic acids in the Cinnamylidene malonic acid crystal structure shows evidence of a new way of hydrogen bonding for dicarboxylic acids. Typically, carboxylic acids will form hydrogen bonded dimers around an inversion center. Dicarboxylic acids will form infinite hydrogen bonded tapes made of these centrosymmetric dimers, with each molecules being related neighboring molecules by the inversion center²³ (Figure 12a,b).

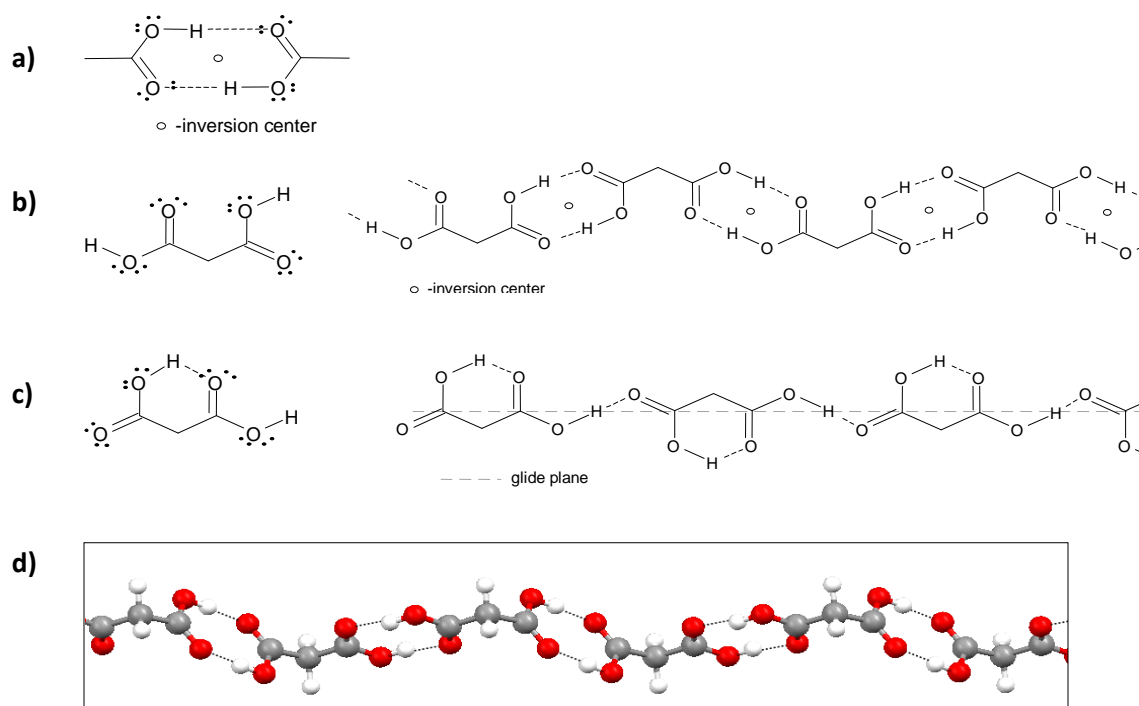


Figure 12: a) typical centrosymmetric dimer H-bonding pattern for carboxylic acids. b). Malonic acid and the hydrogen bond network formed based on the typical carboxylic H-bond synthon. This is the most commonly formed crystal packing found for dicarboxylic acids c) An alternative H-bond pattern for dicarboxylic acids containing an intramolecular H-bond. d). Actual network formed by Malonic acid.

In theory, there is another way that hydrogen binding to occur when the dicarboxylic acid is small and forms intramolecular hydrogen bonds. When a hydrogen is being used intramolecularly, it cannot take part in an intermolecular hydrogen bond dimer formation. When this is the case, carboxylic acids would have to interact in another

way. They may form 1-D hydrogen bonded networks using glide planes or 2- fold screw axis²³ (Fig 12c). We haven't found any examples of this particular type of hydrogen bonding pattern in literature so we cannot further elaborate on it.

Malonic acid forms the predicted hydrogen bonding pattern being that it is a small dicarboxylic acid because each of its carboxylic acids have a favorable tilt angle. When it tilts out of the plane, it prevents intramolecular hydrogen bond formation and allows for intermolecular hydrogen bond formation²³ (Fig 12d).

The carboxylic acids in cinnamylidene malonic acid are conjugated to a cinnamyl unit. This allows for the carboxylic acids to remain in the plane of the molecule and makes them more likely to form an intramolecular hydrogen bond. While studying the actual crystal structure it's seen that the cinnamylidene carboxylic acid will form an intramolecular hydrogen bond and not a dimer formation. It does form H-bonded tapes with adjacent molecules related by a 2-fold screw axis (Fig 13). These H-bonded tapes are close packed through Van der Waal forces with adjacent H-bonded tapes related by inversion centers. Figure 13a illustrates the H-bond tape and the glide plane that cinnamylidene malonic acid forms.

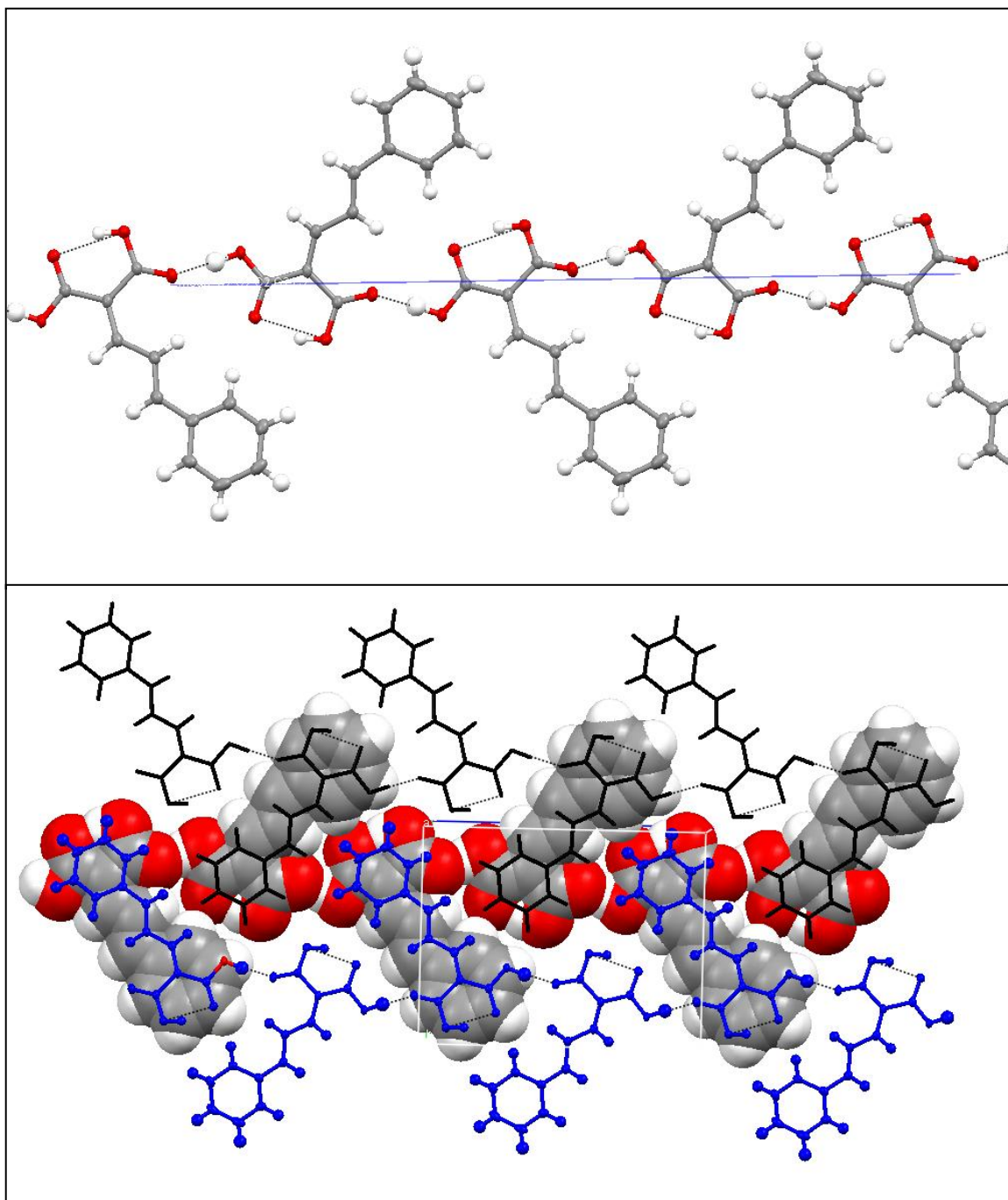


Figure 13: a) The H-bonded tape and the 2-fold screw axis in cinnamylidenemalonic acid. b) Notice here the closeness of the packing in the same molecule

CHAPTER 4: PHOTOCHEMICAL STUDY OF CINNAMYLIDENE MALONIC ACID

4.1: Polymorphs of Cinnamylidenemalonic acid

Originally, the interest was in cinnamylidenemalonic acid being a possible guest compound. It was synthesized because of its ability to hydrogen bond with the host compounds that were to be used. The compound was re-crystallized from ethanol and large crystals formed. It was sent out to retrieve a crystal structure, but was unsuccessful due to being too disordered which suggested that the crystal was undergoing a reaction. It is often difficult to get crystal structures for crystals that undergo solid state reactions. The reaction causes atoms/molecules to move and this creates disorder that prevents structural determination.

During the investigation of the photochemistry of cinnamylidenemalonic acid crystals, a very complicated chemistry was noticed. Initially, there was the fact that cinnamylidene malonic acid crystallized into three polymorphic forms. When each was exposed to UV light, they underwent separate reactions. Two of the polymorphs formed the same [2+2] product while the other formed a complex mixture of products.

Polymorphism is the ability of a solid material to exist in more than one form or crystal structure. Polymorphs can be detected by methods such as melting points, TGA, DSC, and XRD. Data from the XRD indicated that the compound existed in various crystal forms. Figures below illustrate what the crystals looked like under a microscope equipped with a camera and a powder pattern from the XRD (Fig 14).

Here, we were able to retrieve a pattern showing the arrangement of atoms within crystal.

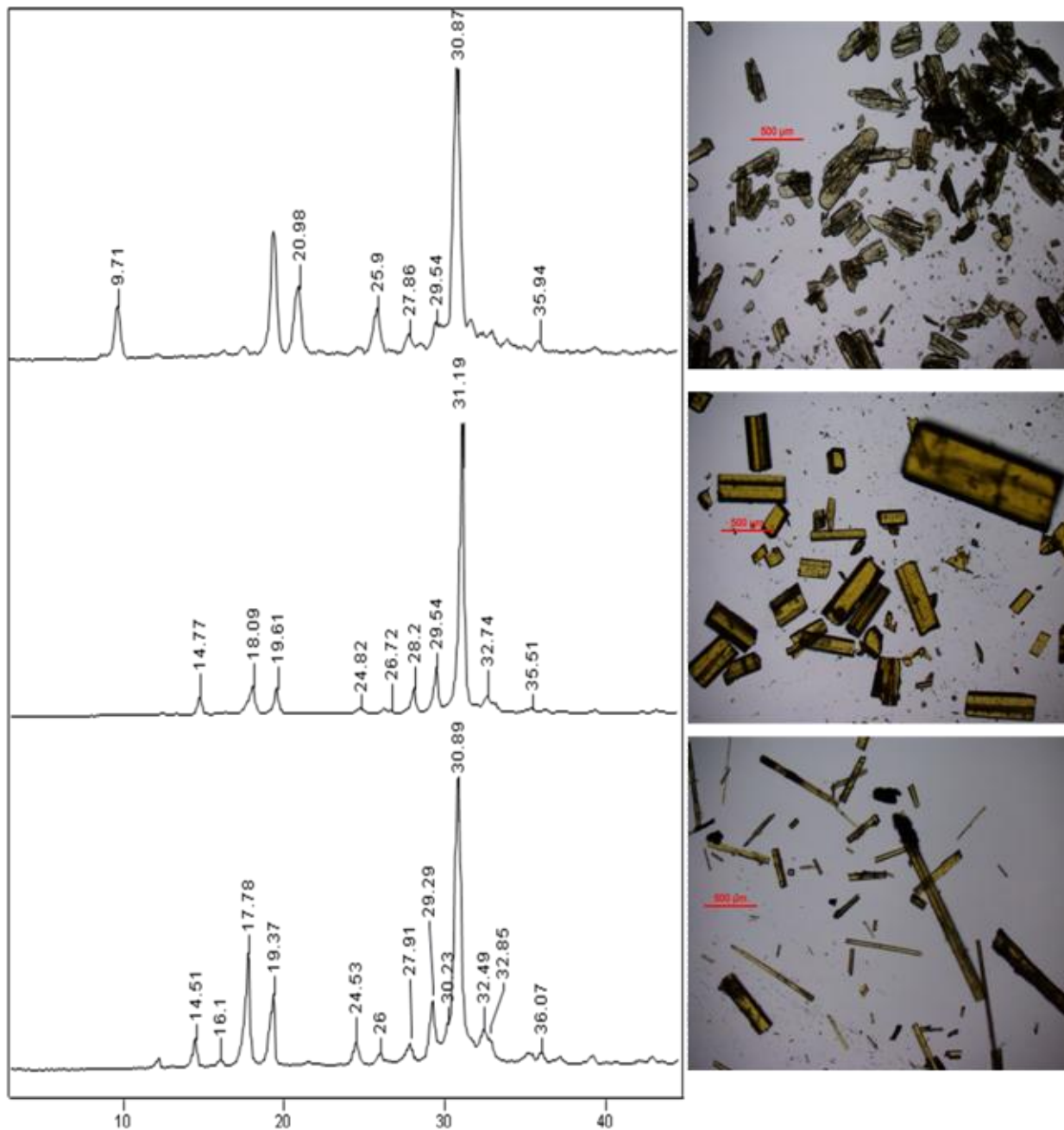


Figure14: Polymorph 1 (top) Polymorph 2 (middle) Polymorph 3 (bottom). Each can undergo reaction when exposed to sunlight or UV light

Each polymorph had a different morphology and X-ray powder pattern.

Polymorph's 1 diffraction pattern is very different from those of polymorph 2 and 3 (Fig 14). The X-ray powder patterns for polymorph 2 and 3 are similar, yet have small differences in peak positions and intensities.

Figure 15 is an illustration of the polymorph 1 and the physical changes upon exposure to sunlight. In figure 15a, the initial sample shows birefringence which indicates crystalline order. Figure 15(a, b) show a decrease in birefringence after three and seven days of sunlight. This is an indication of a loss of crystalline order. The samples appear to have absorbed moisture or melted.

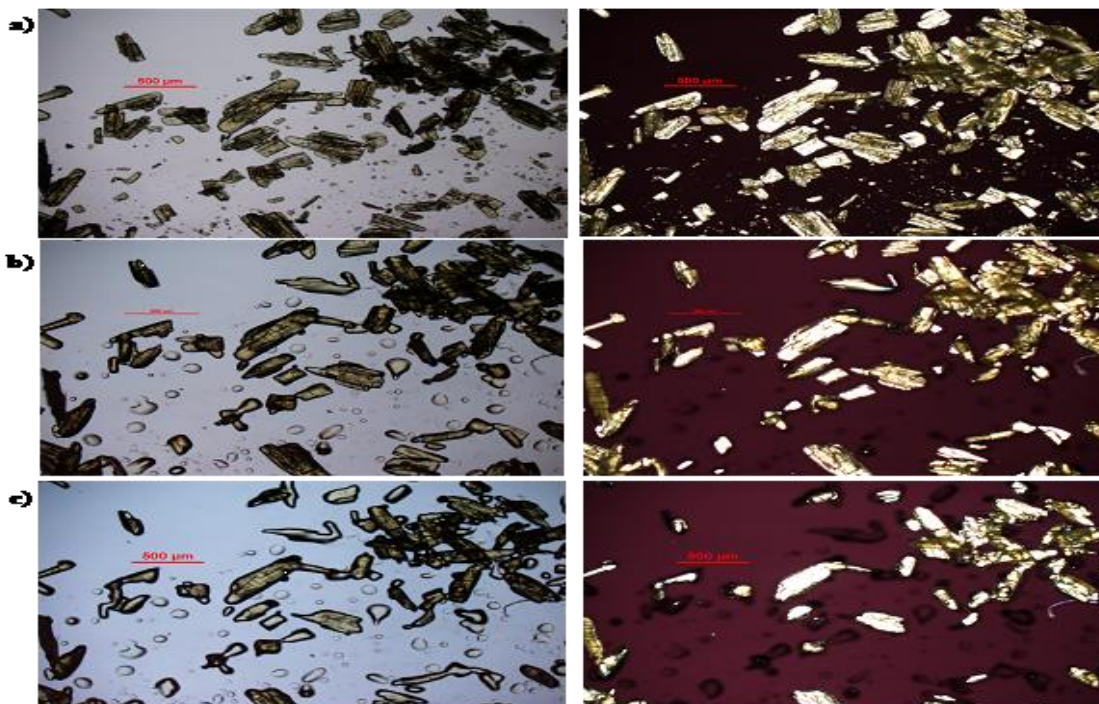


Figure 15: Cinnamylidene malonic acid Polymorph 1 from the jar (stock). left –transmitted light. Right-view with cross polars a) initial b) 3days of sunlight c) 7 days of sunlight. The crystals are losing crystallinity and are either ‘melting’ or absorbing moisture.

Polymorph 2 (Fig 16 a, b) was the first sample that was recrystallized from a solution of ethanol. The photo indicates that it's losing its crystallinity upon exposure to sun light. Small fractures in the crystals could be caused by the reaction itself. The pieces of the fractured crystal still exhibit birefringence under cross polars and indicate that the crystal is still ordered. Since the crystal remains ordered, the topochemical postulate would be in effect because the fractures indicate that the crystal lattice will control the reaction at later stages.

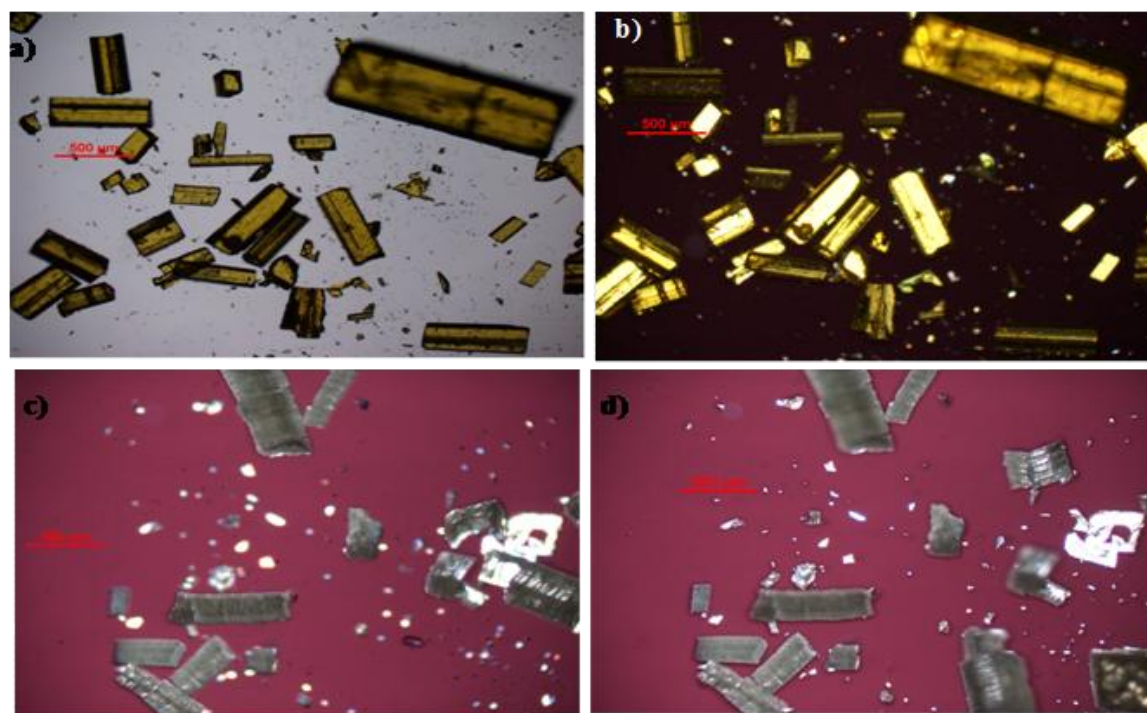


Figure 16: Cinnamylidenemalonic acid polymorph recrystallized from ethanol. a) Initial viewed with transmitted light. b) Initial viewed with crosspolars. c) 3 days of sunlight viewed with crosspolars. d) 7 days of sunlight using crosspolars

Polymorph 3 (Fig 17 a, b) was the last sample that was recrystallized from ethanol. It resembles the 2nd polymorph in its diffraction pattern. This sample also exhibits fractures as small crystals. These crystals also show evidence of double refraction. The topochemical postulate should hold true in this case as well.

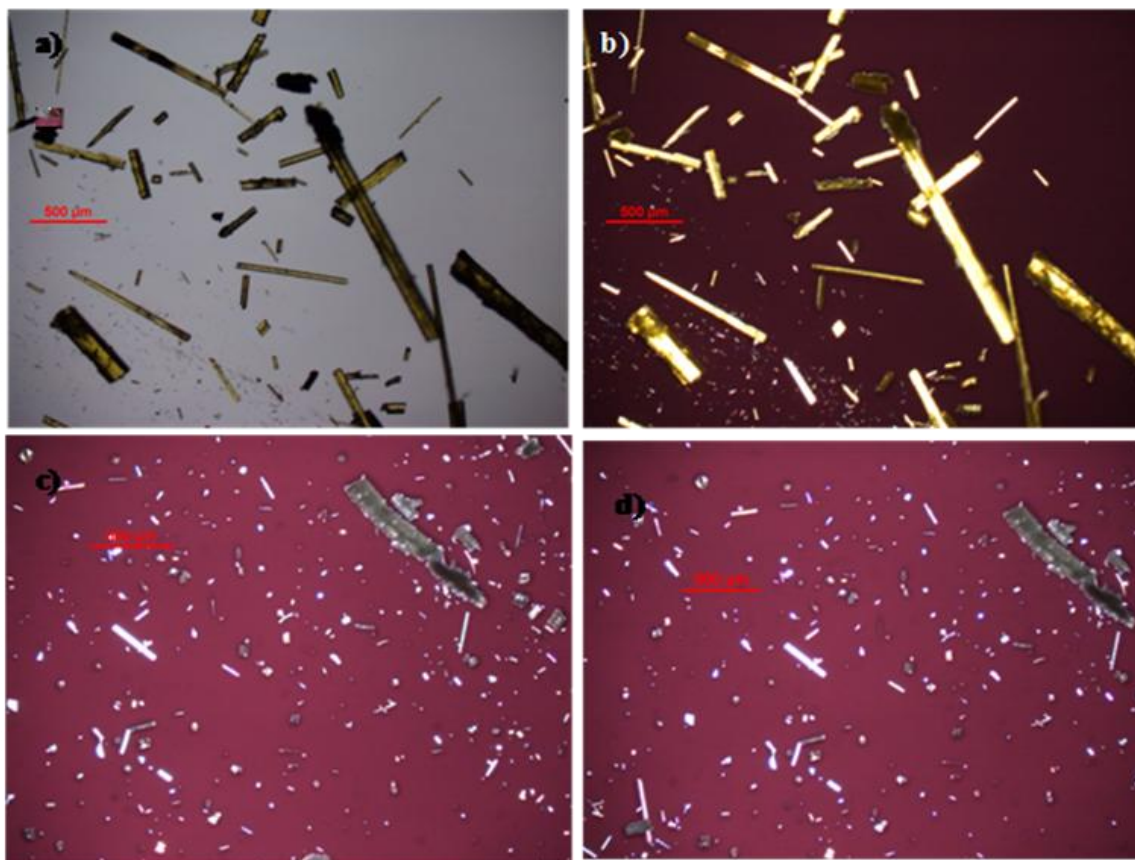


Figure 17: Cinnamylidenemalonic acid polymorph recrystallized from ethanol. a) Initial viewed with transmitted light. b) Initial view with crosspolars. c) 3 days of sunlight viewed with crosspolars. d) 7 days of sunlight using crosspolars.

In figure 18, each of the samples contain partially unreacted starting material and their protons appear in the aromatic region are clearly identifiable by the smaller peaks located at approximately 7.55 ppm. The 2+2 product can be identified by the peaks at ~4ppm because the peaks represent the cyclobutane rings C-H's and the doublet at ~6.5ppm represents the =C-H of the remaining unreacted alkene. Polymorph 1 (fig.18b) produced a complex mixture of products which includes the 2+2 cyclobutane. Figure b shows a large water peak as well as some unidentified peak

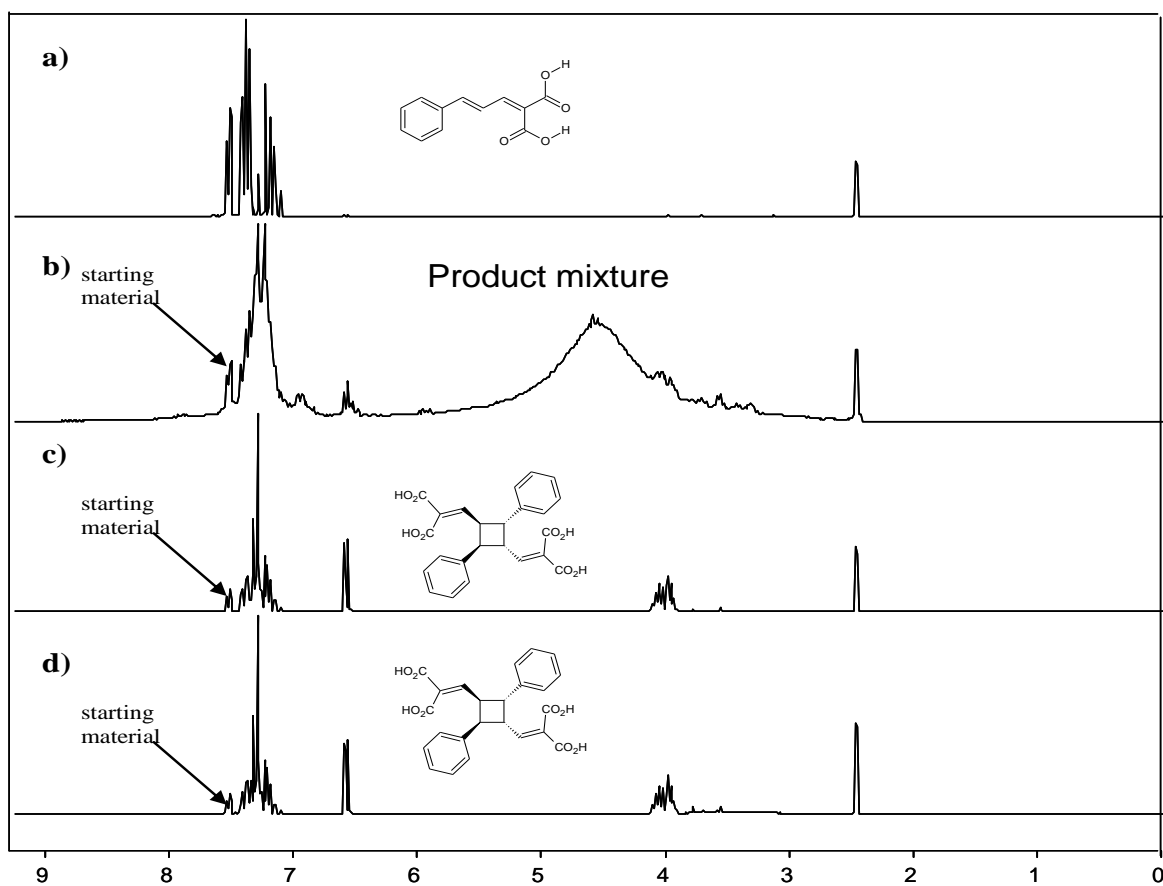


Figure 18: a) Cinnamylidene malonic acid b-d) after 3 days of exposure to sunlight. b) Polymorph 1: product mixture c) Polymorph 2 forms 2+2 product: d) Polymorph 3 forms the same 2+2 product as polymorph 2.

Polymorph 2 and 3 (fig.18 c, d) form the same 2+2 product in high yield impossible since it had absorbed a large amount of water. After 3 days of sunlight,

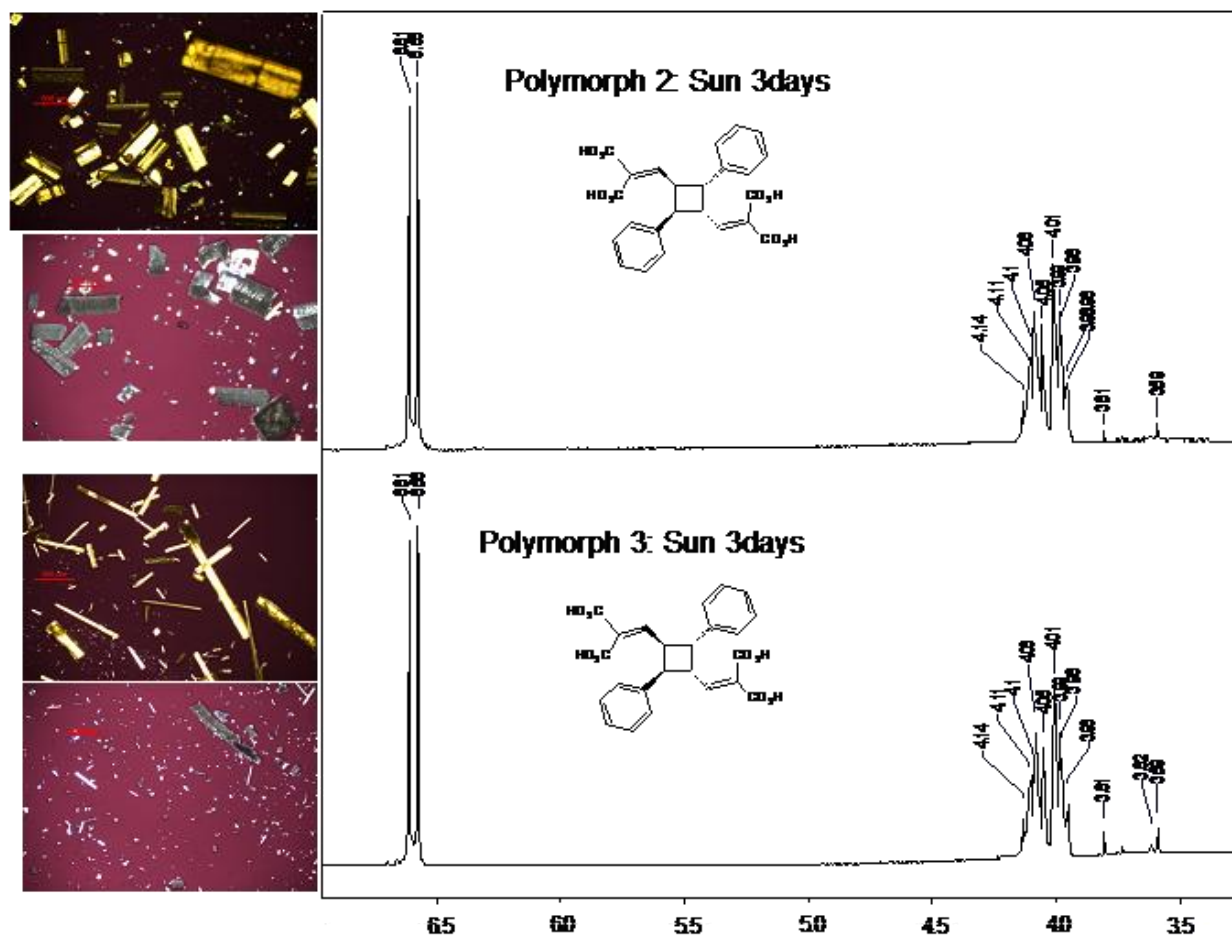


Figure 19: Three days of sunlight. Top: Before and after images of polymorph 2 and ^1H NMR after 3days of sunlight. Bottom: Before and after images of polymorph 3 and ^1H NMR after 3days of sunlight.

Figure 19 shows a closer look at the HNMR of Polymorph's 2 and 3. The peaks at approximately 6.6 ppm represent the two hydrogen's on the alkene while the complex multiplets around 4.1 and 3.98 ppm are complicated but show the four hydrogen's on the

cyclobutane ring with the integration being 2:2:2. The peaks that are around 3.5ppm are unidentified side products and are not part of the actual 2+2 structure.

Most of the attention was focused on polymorph 2 because of the crystal structure that was obtained. When it was irradiated, it gave further proof that the structure was that of a cyclobutane.

CHAPTER 5

KINETICS STUDY OF THE [2+2] DIMERIZATION OF CINNA MYLIDENEMALONIC ACID

5.1: Introduction to Kinetics Study

For [2+2] photodimerizations, the ideal orientation for the best pi-orbital overlap is when the reacting double bonds to be collinear. Figure 20 is an illustration of the best orientation that will allow for a [2+2] cycloaddition.

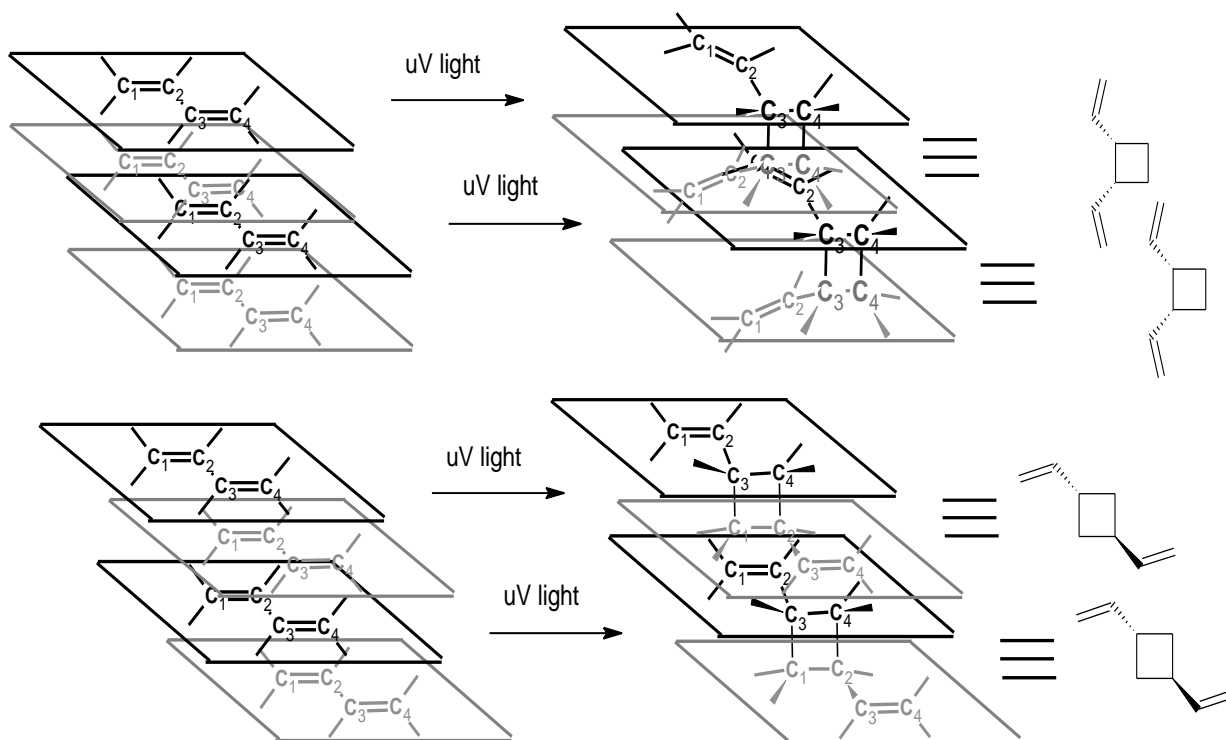


Figure 20: This diagram illustrates the packing parameters that are necessary for 2+2 cyclization as well as the regioselectivity. The diene will lie directly on top of one another and are parallel to one another and this results in $d_s(C_1-C_1')$ of 3.5-4.6Å with no offset between dienes.

The crystal structure of polymorph 2 was obtained. The molecules of the cinnamylidene malonic acid arranged themselves in an alternating 'head-to-tail' fashion (fig 21). Further investigation of the cinnamylidene malonic acid molecules within the crystal structure suggested two possible reaction pathways with each molecule being related to its nearest neighbor by inversion symmetry.

There are two possible reaction pathways that the cinnamylidenemalonic acid could take. These pathways differ in their spacing and approach angle however, both fall within 4.2 angstroms. It's likely that the 98.33° approach angle will provide better orbital overlap, so this approach is more likely since the pathway taken will be the one that is easiest to maneuver and/or uses the least amount of energy (Fig 21).

Reaction pathway one has an approach angle of approximately 109° and the distance between similar atoms is about 3.597 \AA . The atoms will not be directly on top of one another but instead will be at an angle, so this pathway will be least likely since it has less p- orbital overlap.

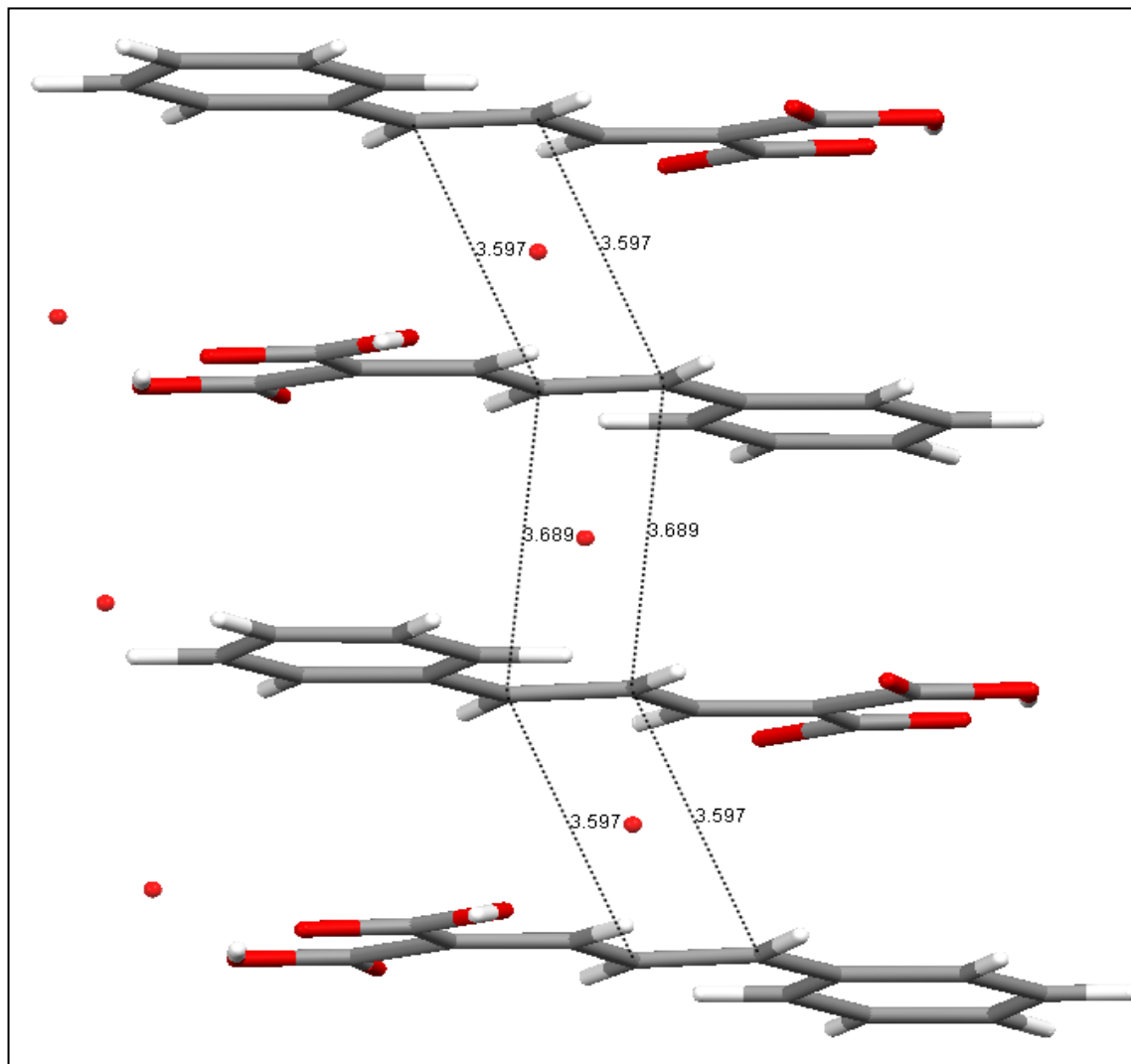


Figure 21: Polymorph 2: 'head-to-tail' stacking pattern of cinnamylidene molecules. Dots indicate inversion centers.

Reaction pathway two has an approach angle is approximately 80 -90 degrees with the distance from similar atoms being about 3.6 angstroms (fig. 22). This pathway is probably more likely since it has greater p orbital overlap. Ultimately, both pathways will ultimately lead to the same product.

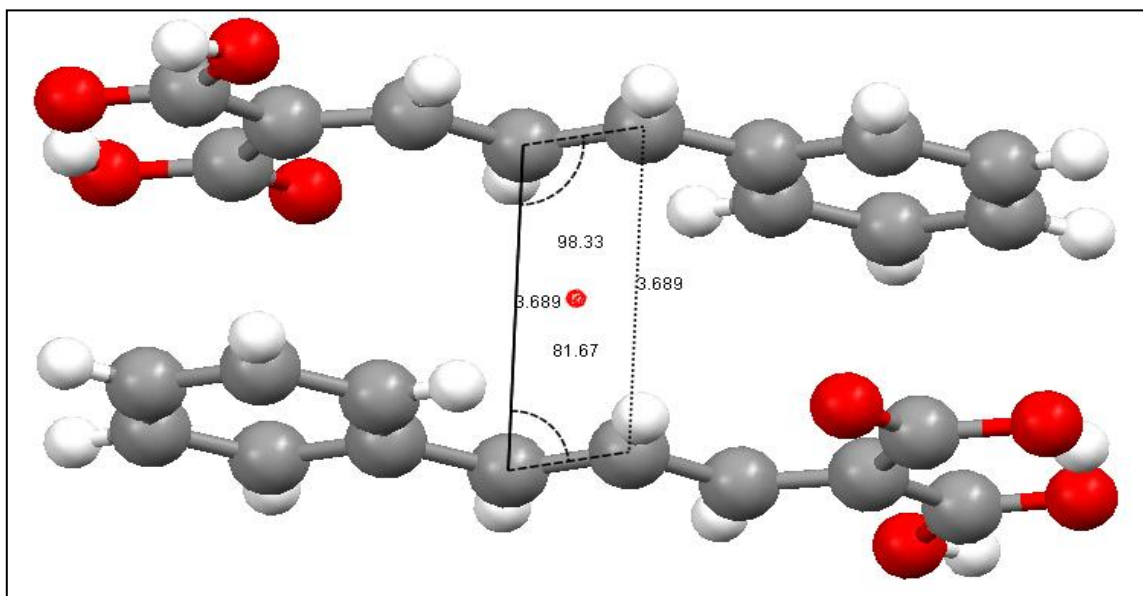


Figure 22: This illustrates a second possible pathway possible with spacing being between 3.689 Å with an approach angle of approximately 98.33°.

Figure 23 illustrates another view of the same methods the molecule could use to stack. Figure 23c, provides evidence of the topochemical postulate due to the fact that the similar atoms lie directly on top of one another leading to minimal movement allowing the lattice to remain in place.

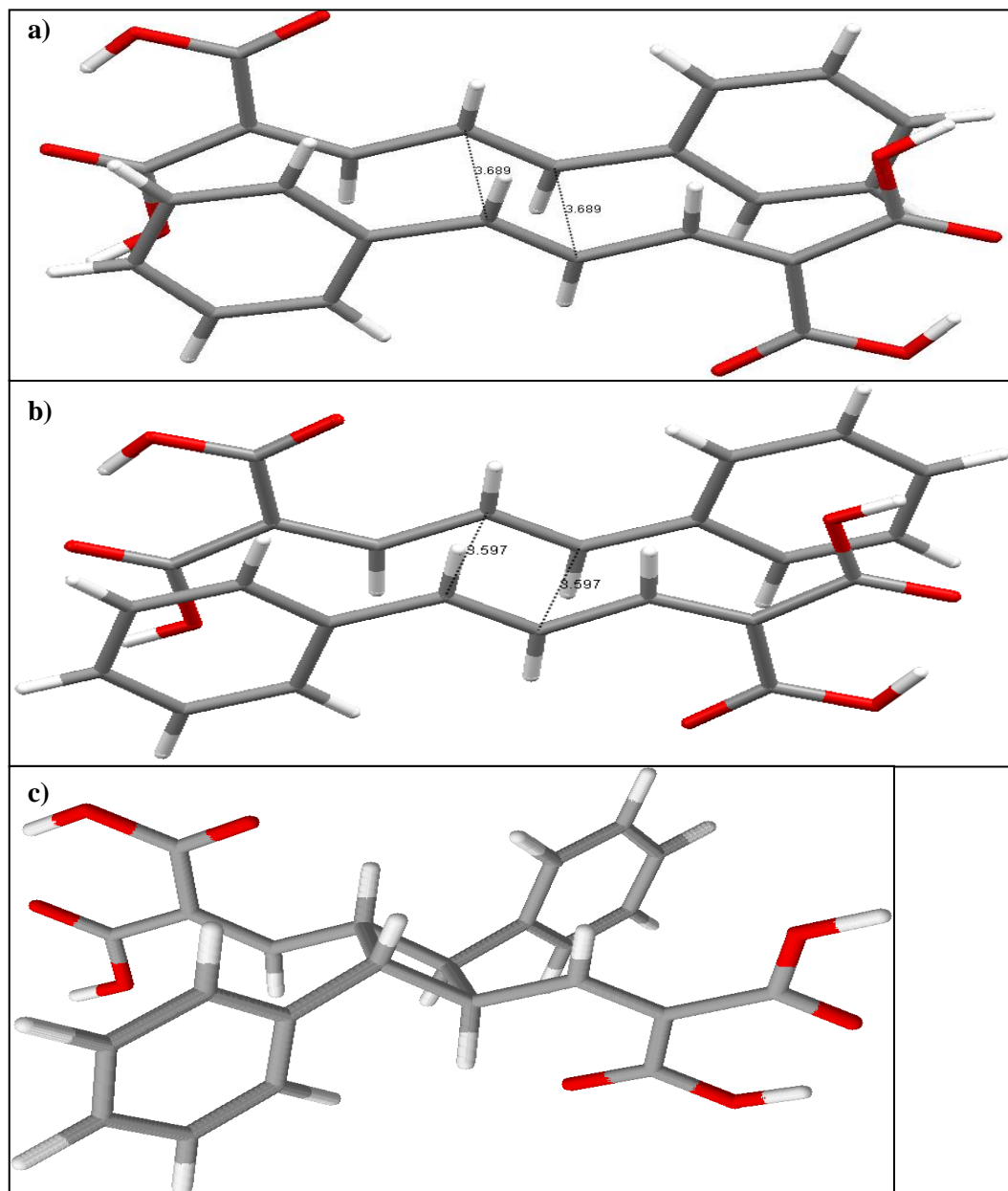


Figure 23: Polymorph 2. a) Reaction pathway one: 3.587 Å separation, 109.19° offset. b) Reaction pathway two: 3.689 Å separation, 98.33° offset. c) Model of product obtained by employing topochemical postulate of least atomic motion. Bonds have been inserted between nearest C atoms. Both reaction pathways produce the same product.

The 2+2 topochemical reaction yield of polymorph 2 was determined by H NMR. The peak at 7.55ppm corresponds to the =C-H alkene hydrogen of the starting material. The hydrogen shifts to approximately 6.6ppm in the final product. Comparing the integration of these peaks helped in determining the percent yield. The peak at 7.55ppm on the left indicates only approximately 28% of unreacted cinnamylidenemalonic acid. The structure on the right indicates a yield of about 72% of a 2+2 product with 28% being unreacted cinnamylidenemalonic acid (Fig 24).

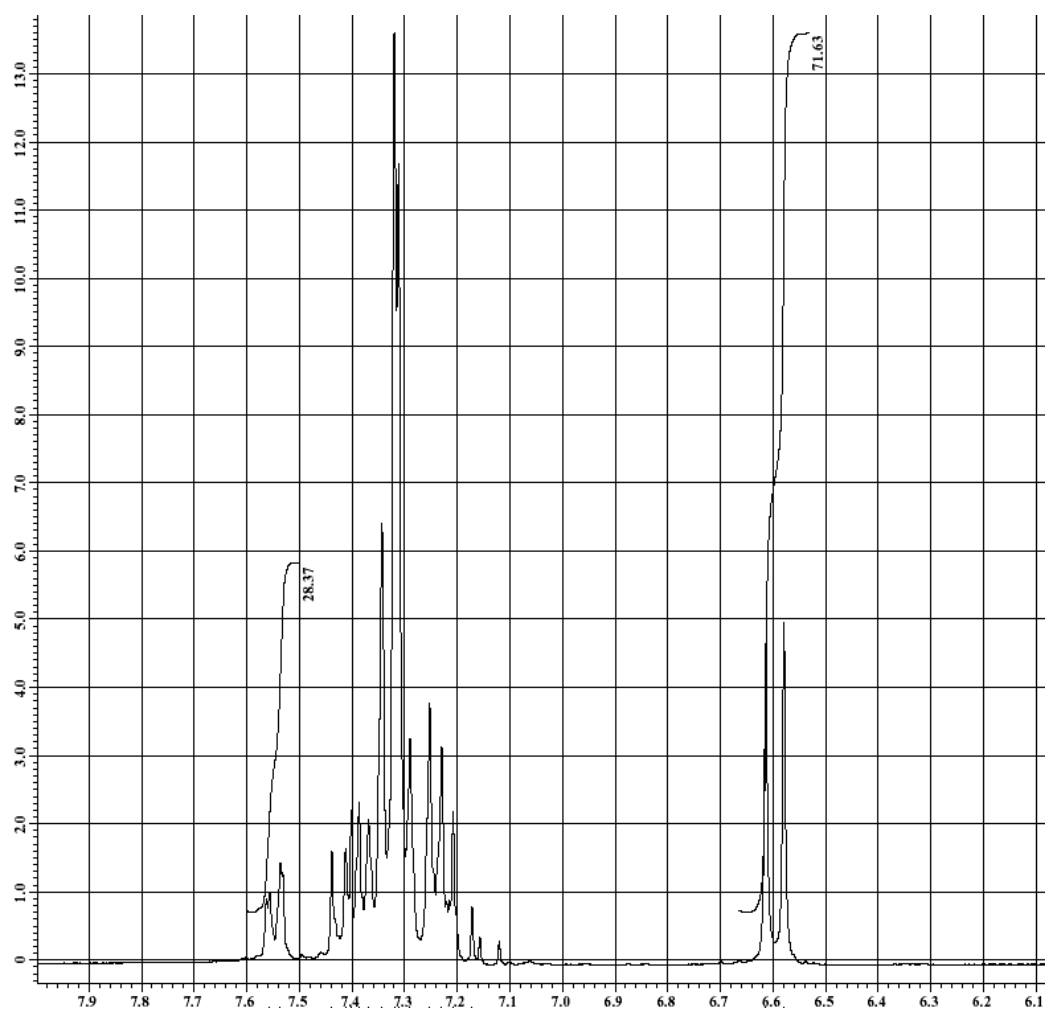


Figure 24: NMR representing a sample exposed to sunlight for 3 days.

With the compound being symmetrical, the number of carbon signals in the molecule should be eight (Fig 25). There are eight peaks in the spectrum each representing the number of carbon atoms with the smaller unlabeled peaks representing unreacted starting material. Peaks located between 150-120 ppm relate to the alkene carbons. Peaks located between 210-160 ppm relate to the carboxylic acid carbons. Peaks located between 40 and 50 ppm relate to carbons in the cyclobutane ring. This information was obtained by literature³⁰.

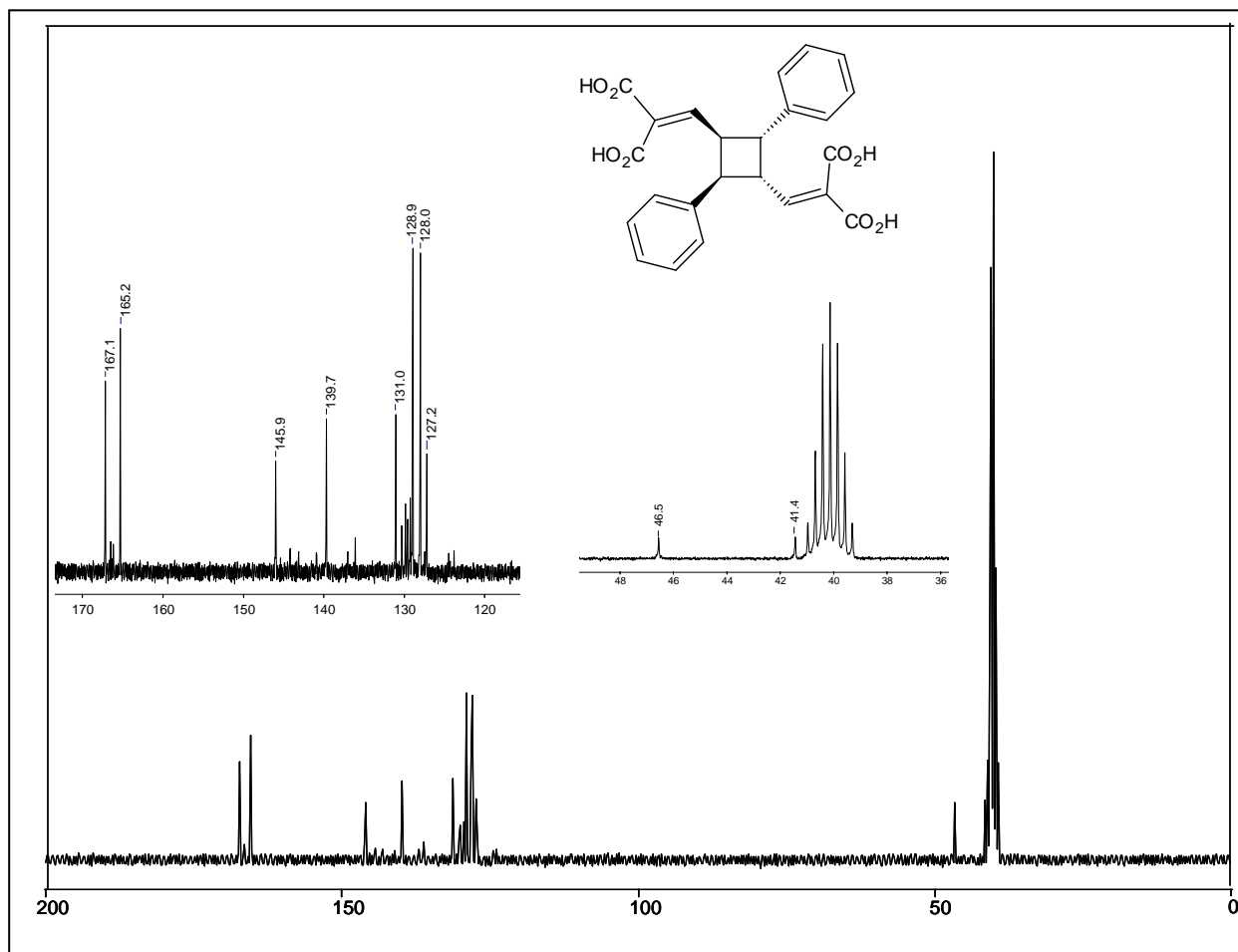
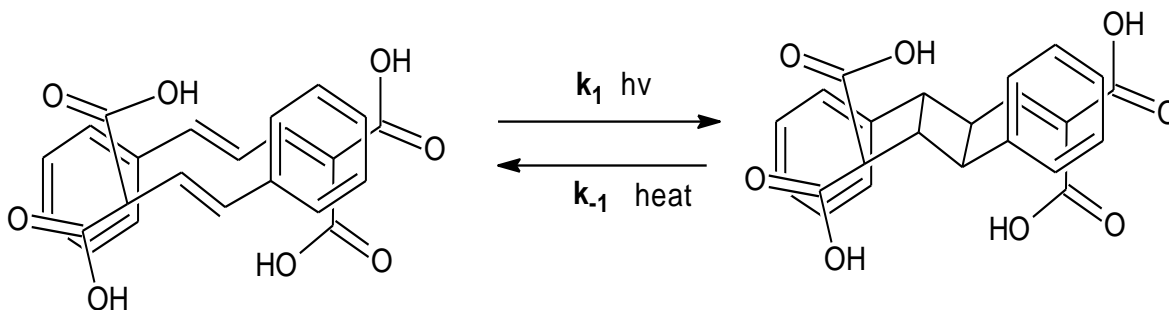


Figure 25: ^{13}C of the predicted structure.

5.2 Kinetics Study Results



Scheme 4: Illustration of cinnamylidene malonic acid as it reacts with UV light. This reaction can be reversible.

The goal here was to work on methods to study the kinetics of solid state reactions. These methods were to be developed and applied to other solid state reactions that were being studied in the research group. Many difficulties were encountered during the project that allowed for only a small number of successes. What follows is a description of those methods along with the difficulties that were encountered.

2+2 dimerization is forbidden thermally however is allowed photochemically (scheme 4). Light will cause the 2+2 reaction to happen while heat present will not. The ring opening of the cyclobutane ring is allowed thermally and when heated without light will allow the reaction to be undone.

There are, of course, some complications to the kinetic study. For instance, the rate law would be $\text{Rate} = k_1 [\text{monomer}]^x - k_{-1} [\text{dimer}]^y$. For this particular case there is no integrated rate law because there is no simple form to define. When the reaction is at its early stages, the dimer is low and the rate law can be assumed to be $\text{Rate} = k_1 [\text{monomer}]^x$. Using this assumption, attempts were made, however unsuccessfully, to

find (X) using the regression analysis and the integrated rate law to see if (X) was zero, first or second order.

A second complication is that there are difficulties measuring the [**monomer**] concentrations and [**dimer**] concentrations, since the reaction occurs within a crystal without a solvent. In this case, it is best to use mole fractions instead (x_{monomer} and x_{dimer}). The method that was used to determine the mole fractions was a method that was used by other groups¹ and by studying their similar reaction predictions. The IR bands in our spectra were highly overlapped and were difficult to interpret making it almost impossible to measure the concentrations of the dimer and the monomer.

5.3 Kinetics Study Using FTIR/ATR

The goal was to understand the kinetics involved in the photochemical reaction of Cinnamylidene Malonic acid (polymorph 1). The interest was in what rate the monomer was converting to the dimer. The experiment consisted of preparing a BaF₂ and Cinnamylidene Malonic acid into a pellet and placing it into the UV photoreactor. The average temperature within the reactor was 23.7°C. It was then placed in the FTIR/ATR for analysis. This procedure was repeated several times over a period of approximately 400 minutes. The spectra that were obtained were baseline corrected as well as normalized. Bands that were increasing were those that attributed to the dimer while bands that were decreasing belonged to the monomer. Using the FTIR/ATR, wavenumbers were normalized and baseline corrected in order to place the peaks on top of one another, which allows for an accurate measure of which peaks are growing and which ones are disappearing. Any peaks that appear to be shrinking would represent

those of the monomer while ones that appear to be growing would represent dimer formation. The wavelengths that give the best example of what the goal of the project is are the ones located at 700cm^{-1} and 716cm^{-1} (Fig 26). Monomer and dimer bands were highly overlapped and it is difficult to analyze the data in these particular spectra.

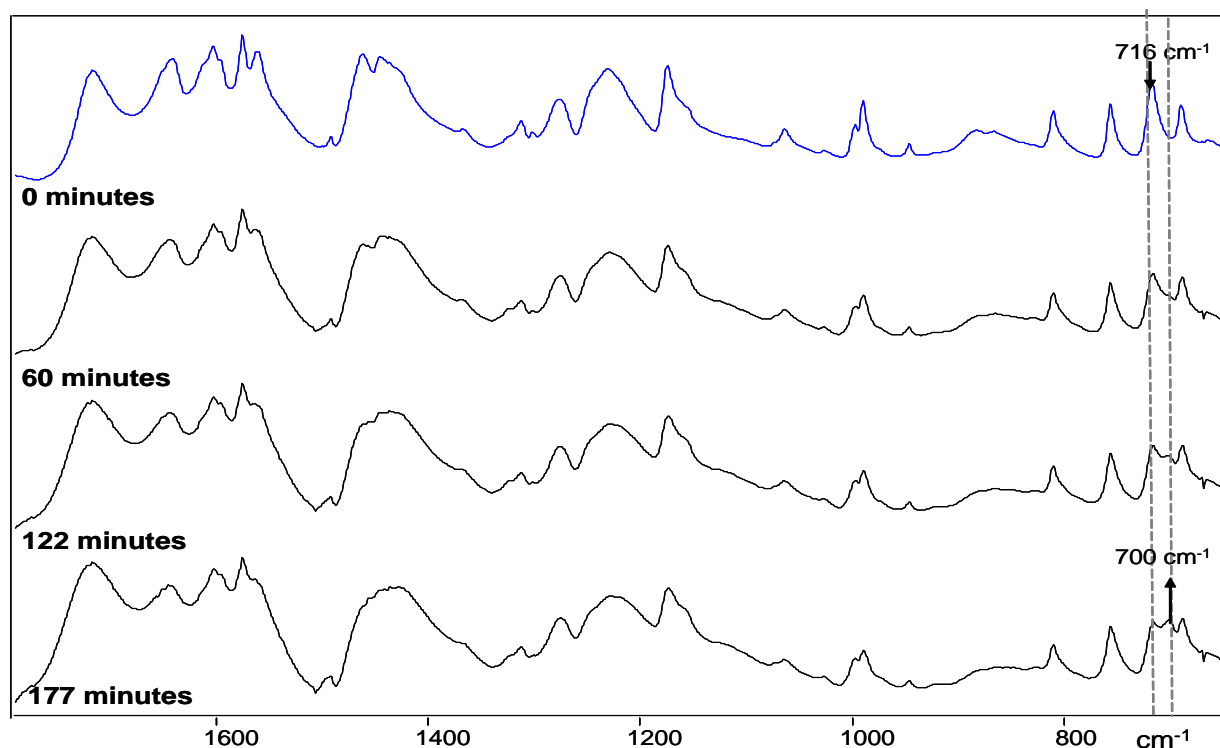


Figure 26: Representation of the Infrared of polymorph 2 over a period of 177 min.

Figure 27 more clearly illustrates the most obvious changes in the infrared spectra of the photochemical 2+2 reaction. The most obvious changes occur at 716 and 700 cm^{-1} . According to Beers law, the concentration of the monomer and the dimer are proportional to the absorbance of these bands in the IR.

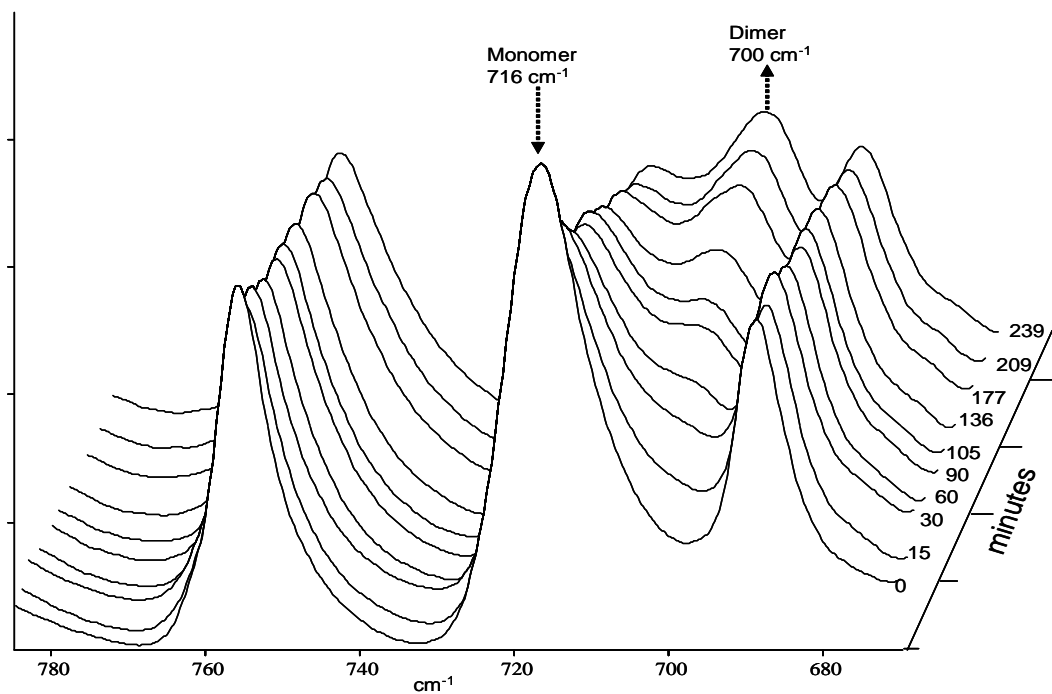


Figure 27 : Illustration of the monomer and dimer: $A_m = \epsilon_m b [\text{monomer}]$ and $A_d = \epsilon_d b [\text{dimer}]$.

The method described by Matsomoto et.al. was used to calculate mole fraction of monomer and dimer during the course of the reaction.¹ The molar absorptivity of the sample changes during the reaction. Molar absorptivity is a measure of how strongly a chemical species absorbs light at a given wavelength.

To correct for this change, the molar absorptivity of the monomer 716 cm^{-1} band was plotted against that 700 cm^{-1} band of the dimer. The slope of this line was used as a correction factor and corrected for the changing the molar absorption.

Many formulas were implemented in order to obtain the data needed to confirm whether the plot of the monomer versus the product would show whether the reaction

was zero, first or second order. The mole fractions were calculated mathematically using equation 4. (table 4)

EQUATION	VALUE OBTAINED
1 $A_1 = \epsilon_1 b X_1$	Reactant Concentration
2 $A_2 = \epsilon_2 b X_1$	Product Concentration
3 $A_2 = -(\epsilon_2/\epsilon_1)A_1 + \epsilon_2 b$	Plot produces a straight line with slope = ϵ_2/ϵ_1 . This is the correction factor for the change in molar absorptivity.
4 $x_1 = 1/\{(A_2/A_1)(\epsilon_1/\epsilon_2) + 1\}$	Equation derived from equations 1-3 to find the monomer mole fraction.

Table 4: Subscripts 1 and 2 represent monomer and dimer respectively. X represents mole fraction, b represents path length, e represents molar absorptivity.

Difficulties in this IR study led to the decision to study the reaction further using H^1 NMR. The reaction did not follow a zero, first or second order rate law. These values were plotted to determine which rate law best fits the reaction. Solid state reactions usually follow a first order rate law³². This is what was expected in this study, however, when the values were finally plotted they did not seem to follow any one particular rate law. There were many issues with this study with one being that the samples were not collected on the same day. This allows for the reaction to proceed backwards and revert back to the monomer. The spectra that follow represent the data collected and interpreted.

TIME (MIN)	716.73 CM-1 MONOMER	700 CM-1 DIMER	MONOMER mole fraction	Ln (x)	1/x
0	1.32	0.58	1.00	0.00	1.00
15	1.15	0.65	0.91	-0.10	1.10
30	1.11	0.73	0.85	-0.16	1.17
45	1.10	0.78	0.82	-0.19	1.22
60	1.06	0.80	0.80	-0.22	1.25
75	1.04	0.83	0.78	-0.25	1.29
90	1.03	0.88	0.75	-0.29	1.33
105	1.02	0.89	0.74	-0.30	1.35
121	1.03	0.94	0.73	-0.32	1.38
136	1.01	0.96	0.71	-0.34	1.41
177	0.96	0.99	0.68	-0.39	1.47
209	0.93	1.01	0.65	-0.43	1.54
239	0.94	1.06	0.65	-0.44	1.55
271	0.89	1.05	0.63	-0.46	1.59
301	0.89	1.09	0.61	-0.49	1.63
337	0.84	1.08	0.60	-0.52	1.68
373	0.83	1.10	0.59	-0.53	1.71
409	0.82	1.12	0.58	-0.55	1.74

Table 5: Table of Calculated Mole Fractions.

The mole fractions that were calculated were plotted several times in order to determine whether the reaction fit a zero, first or second order reaction. The data collected was plotted and the graph that follows represents another attempt to find which rate law the reaction best fits.

A zero order reaction, the rate would be constant. It would not change with concentration.³² (Fig 28)

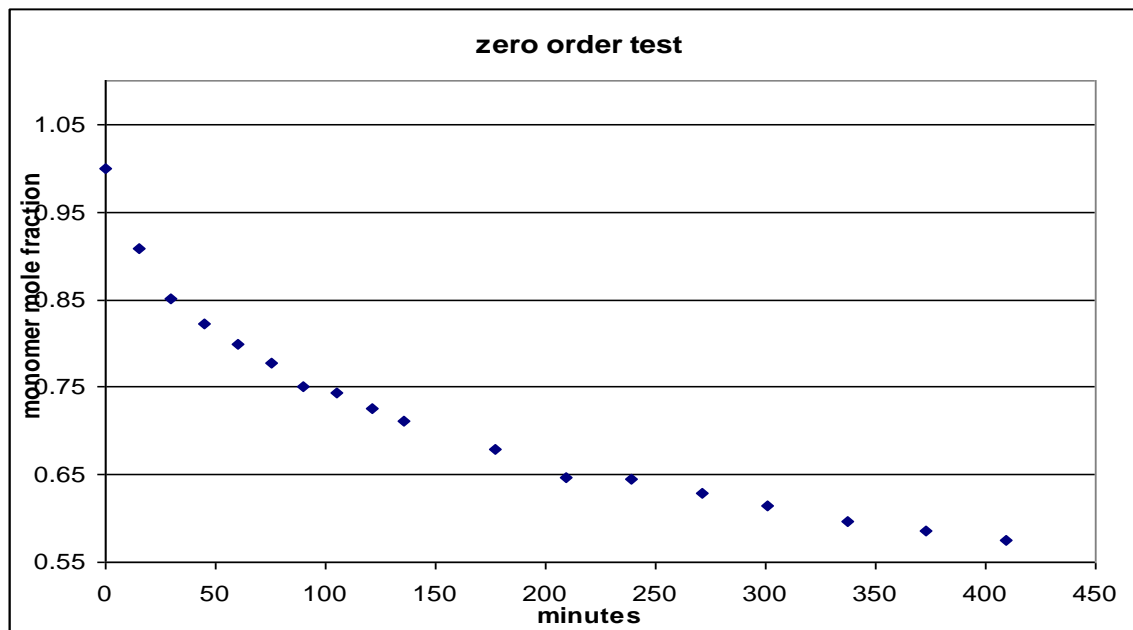


Figure 28: This graph represents the mole fraction versus a change over time. It should be linear so it does not fit a zero order reaction. The integrated rate law for this reaction would be $[A] = -kt + [A]_0$.

For a first order reaction, a plot of the $\ln[X]$ should produce a straight line.

Figure 29 indicated that the data did not fit a first order reaction.

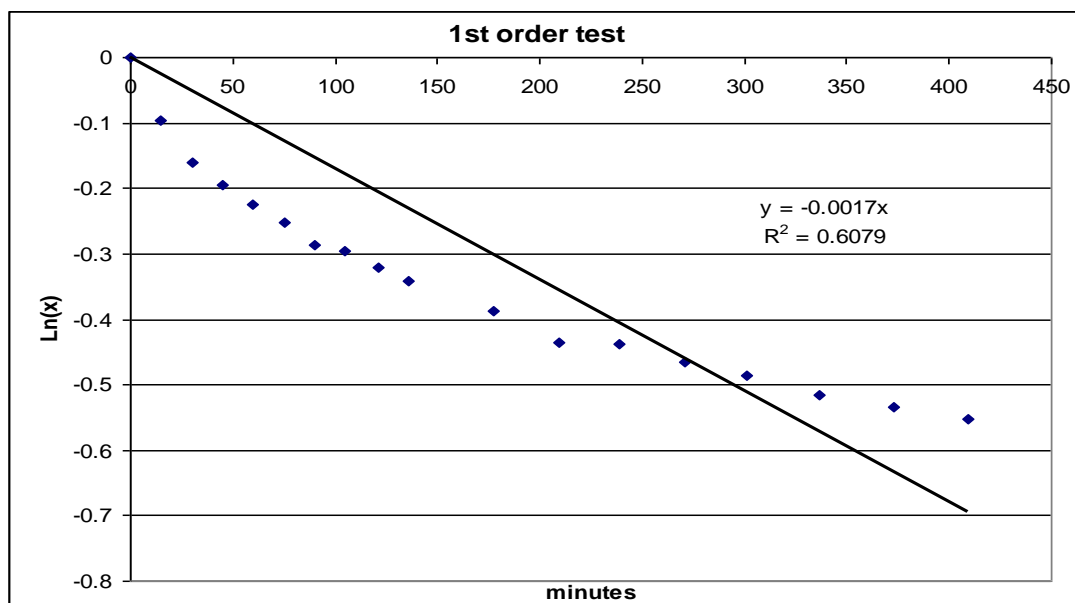


Figure 29: Illustration of the data plotted in an attempt to find a suitable rate law. This data does not fit a typical 1st order reaction.

A second order rate law states that $1/[x]$ versus time should produce a straight line.

The data that was collected does not illustrate a second order reaction either. (Fig 30)

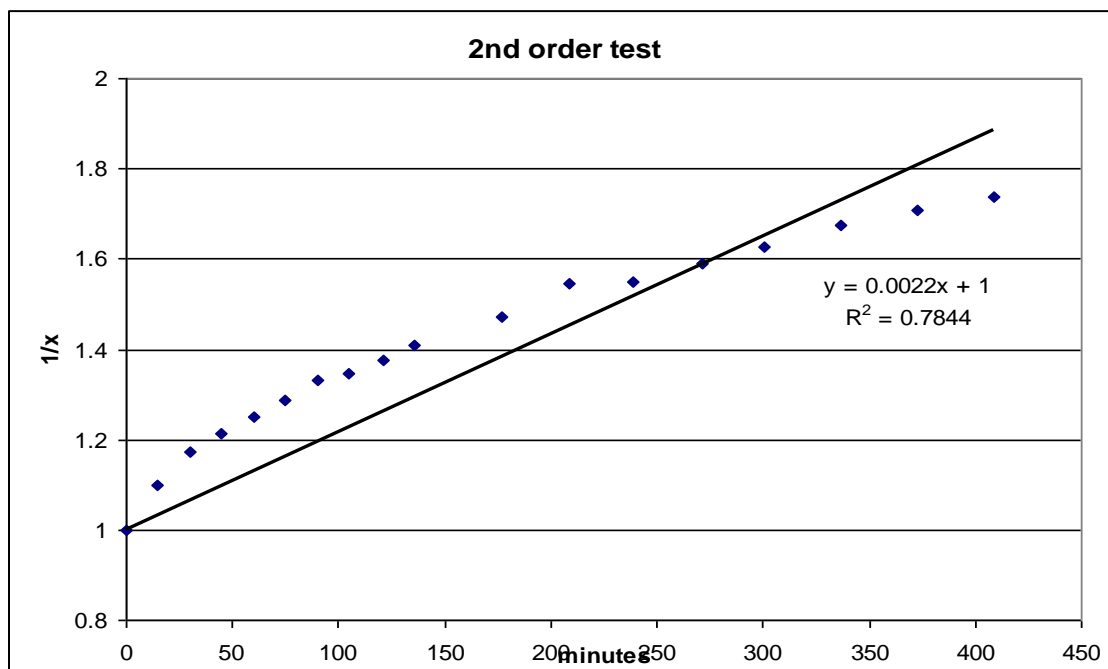


Figure 30: A plot of $1/[x]$ should be linear, however, this data proves not to produce a straight line and is therefore not a 2nd order reaction.

After conducting this kinetic study, it was discovered that polymorph 1 of cinnamylidenemalonic acid produces multiple products and there are multiple reactions occurring. The occurrence of multiple reaction pathways occurring simultaneously results in an overall rate law with a fractional order. It proved very difficult to obtain any useable information from this data.

We then turned our attention to studying the kinetics of the 2+2 photoreaction of polymorph 2 which produces only one product. The research was continued using this polymorph and the photochemical reaction was studied using the H^1 NMR.

5.4 Kinetics Study using H^1 NMR

The goal of this study was again to understand the kinetics of the photochemical reaction of Cinnamylidene Malonic acid. Instead of producing a BaF_2 pellet, the sample was put in a quartz round bottom containing hexanes. The hexanes were chosen because of its inability to absorb UV light, therefore allowing more of the light to be absorbed by the compound itself. This solution was placed in a UV box for various times and then taken for H^1 NMR analysis. There were some difficulties in controlling the temperature. During the experiment, the temperature ranged from 39-40 °C with an average temperature of 41°C. The quartz reaction vessel was kept at 40° C when it was not in the photoreactor. NMR samples were collected over a number of time intervals by vacuum filtration, dried and dissolved in d_6 DMSO. NMR samples were protected from ambient light.

Figure 31 shows the changes that were monitored in the H^1 NMR spectra. The peak at 6.7 ppm corresponds to the =C-H for the dimer product. All of the proton

signals for the monomer appear from 7.0-7.8 ppm. Mole fractions for the monomer and the dimer were solved algebraically based on the integration at peak 6.7 and the area under the aromatic region.

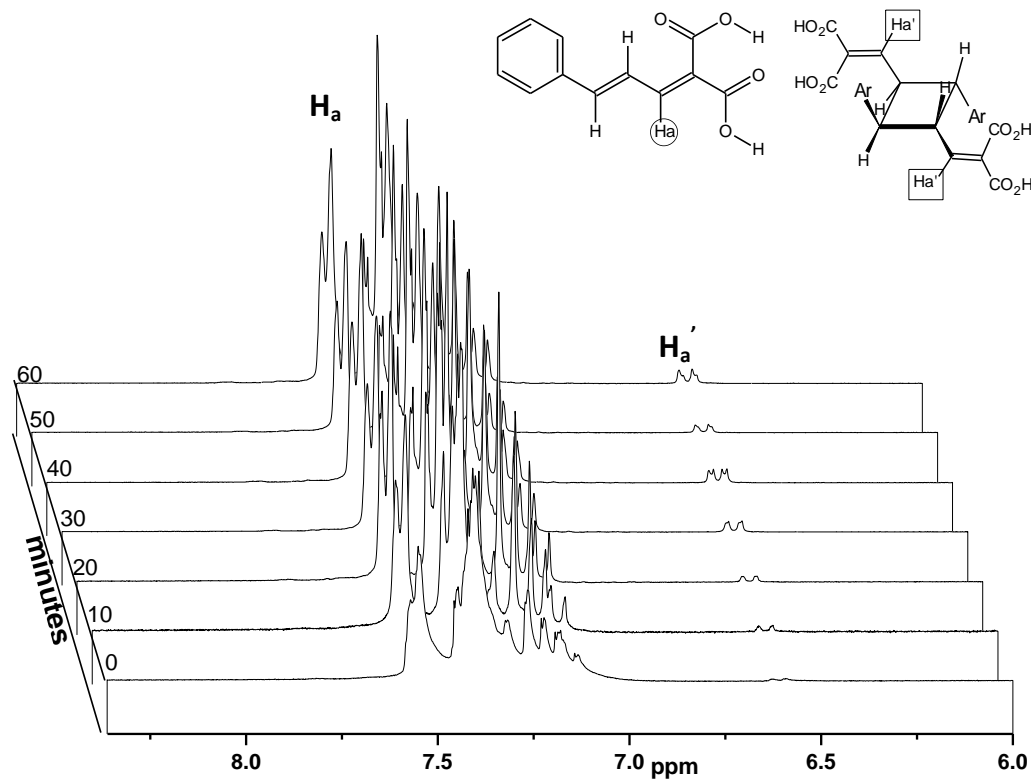
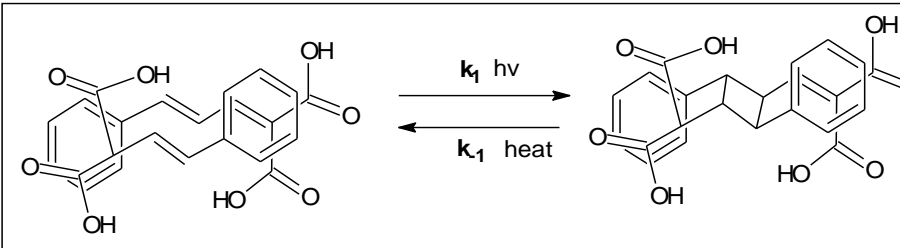


Figure 31: NMR illustration of the changes over time occurring in both the aromatic region (7.0-7.5 ppm) as well as the alkene region (6.5-7.0 ppm).

We were not able to determine a reasonable rate law from the NMR data. The mole fraction of monomer and dimer based on H^1 NMR did not decrease continuously. It can be seen in table 5 that the monomer concentration actually increases at certain time intervals. This may be caused by extended time intervals between isolating a samples

and collecting its NMR spectra. The time interval between isolating a sample and collecting its NMR spectra may have allowed for the thermally allowed reverse reaction to occur. Another possible cause of this behavior is that the reaction was monitored over multiple days. This would also allow time for the reverse reaction to occur.



date sample collected	date NMR collected	time minutes	mole fract monomer x	LN(x)	1/x
31-Aug	7-Sep	0	0.980	-0.020	1.020
31-Aug	1-Sep	10	0.979	-0.021	1.022
31-Aug	3-Sep	20	0.977	-0.024	1.024
31-Aug	3-Sep	30	0.948	-0.053	1.054
31-Aug	3-Sep	40	0.937	-0.065	1.067
31-Aug	3-Sep	50	0.957	-0.044	1.045
31-Aug	3-Sep	60	0.945	-0.057	1.058
31-Aug	3-Sep	80	0.917	-0.087	1.091
31-Aug	7-Sep	100	0.923	-0.080	1.084
31-Aug	1-Sep	120	0.908	-0.097	1.101
1-Sep	7-Sep	180	0.913	-0.092	1.096
3-Sep	7-Sep	240	0.802	-0.220	1.247
3-Sep	7-Sep	316	0.762	-0.271	1.312
3-Sep	7-Sep	376	0.719	-0.330	1.390
6-Sep	7-Sep	430	0.738	-0.304	1.355
7-Sep	7-Sep	654	0.786	-0.240	1.272

Table 6: Table of mole fractions calculated. Those highlighted in yellow represent changes that represent dimer converted back to monomer.

Calculating a rate of the reaction was unsuccessful for a few reasons, one being that the samples taken for H^1 NMR were not consistent in the times that they were collected.(table 6) When the samples sat they were able to revert back to the monomer therefore hindering results that would be meaningful to the study.

CHAPTER 6: EXPERIMENTALS

All reagents were purchased from Aldrich or Acros and used without further purification unless otherwise noted. All reported melting points are uncorrected. NMR spectra were recorded on a JEOL Delta 300MHz spectrometer in CDCl₃ or DMSO-D₆. IR spectra were obtained on Perkin Elmer SpectrumOne spectrometer with a Universal ATR attachment. UV-Vis measurements were measured on a HP 8453 Ultraviolet – Visible Spectroscopy (UV-Vis) spectrometer. X-ray powder patterns were collected on the Rigaku MiniFlex XRD. Single crystal X-ray structures were obtained on Bruker SMART APEX II: 4K CCD System with 3-circle goniometer equipped with an Oxford Cryostream Plus variable temperature controller. Crystallographic data was collected by Dr. Robert Pike and James Jones at the College of William and Mary. The crystal structures were solved using ShellX and SaintTM software and the structures were illustrated using HgTM software. Photographs of crystals were recorded using a Nikon Labophot Pol - Binocular Polarizing microscope. Photochemical reactions were conducted using a Rayonet photochemical reactor fitted with 254 nm lamps.

Dimethyl Tartrate³⁴ [S,S] D (+) Tartaric acid (66.6 mmol), Boric acid (48.5 mmol), and dry Methanol (150 ml) were added to a reaction vessel and allowed to stir without heat for 22 hours. The resulting solution was placed under reduced pressure resulting in a light yellow viscous solution. Yield (9.15g, 77.14%). MP/BP: 57-60 °C (dec)/163°C. ¹H NMR (CDCl₃, 300MHz): δ = δ 3.4ppm (s, 3H), δ 3.8ppm (s, 2H), δ 4.5ppm (s, 1H). FTIR (ATR): 3442 cm⁻¹ ,1733 cm⁻¹ ,1438 cm⁻¹ ,1226 cm⁻¹ ,1126 cm⁻¹ ,1083 cm⁻¹ , 975 cm⁻¹ .

N,N'-bis(pyridine-4-ylmethyl) D-(S,S)-Tartaramide³⁵ D-Dimethyl Tartrate [S, S] (1.0 g, 5.6mmol), 4-(aminomethyl) pyridine (1.4 ml, 12.6 mmol) and potassium carbonate(.27g .2mmol)and (10ml, 33.38ml/1ml) of Methanol was added to a reaction vessel and allowed to reflux 1-3 hours to yield an orange solid material. This was vacuum filtered and washed with methanol to yield a white solid followed by recrystallization in 2:1 Methanol and Ethyl Acetate. Yield: (.621g 33.5 %). Mp: 210-212°C. ¹H NMR (d₆ DMSO, 300MHz): δ 8.8 (ddd, 2H), δ 7.15 (ddd,2 H), δ 5.9(s, 1H), δ 4.6(s,2H) , δ 3.4 (s, 2H) ppm. ¹³C NMR (d₆ DMSO, 300MHz): δ = 173, 149, 150, 122, 123, 74, 40... ppm. FTIR (ATR): 3031, 1748, 1601, 1416, 1217, 1096, 1139....cm⁻¹.

N,N'-bis(pyridine-3-ylmethyl) D-(S,S)-Tartaramide³⁵. D-Dimethyl Tartrate [S, S] (1g, 5.6 mmol), 3-(aminomethyl) pyridine (1.4ml, 12.6 mmol), Potassium Carbonate (.27g, 0.2 mmol) and methanol (10ml, 3.38ml/1ml) were added to a reaction vessel and allowed to reflux for 1-3 hours to yield an orange solid material. An additional amount of methanol was added and the reaction was allowed to reflux for an additional 30 min to

yield a light orange solid. This was then vacuum filtered and washed with Methanol. The resulting white power was recrystallized in a 4:1 mix of Methanol and Ethyl Acetate, hot filtered and allowed to cool to room temp to afford a crystalline material. Yield (0.25g, 13%) MP=182°C. ¹H NMR (d₆ DMSO, 300MHz): δ = 8.5 (ddd,1H), δ 8.4 (ddd 1H), δ 7.7 (ddd, 1H), δ 4.55 (d, 1H), δ 4.54 (d,2H). ¹³C NMR (d₆ DMSO, 300MHz): δ= 172.9, δ 149.19, δ 148.41, δ 135.59, δ 135.43, δ 123.82 ppm. FT/IR (ATR): 3308, 1641, 1681, 1527, 1419, 1332, 1278 cm⁻¹.

N,N'-bis(pyridine-2-ylmethyl) D-(S,S)-Tartaramide³⁵. Dimethyl Tartrate [S, S] (1.0g, 5.6 mmol), 2-(aminomethyl) pyridine (1.6ml, 12.6 mmol), potassium carbonate (.27g 0.2 mmol) and methanol 10 ml (3.38ml/1ml) were added to a reaction vessel and allowed to reflux for 1-3 hours to yield an orange solid material. An additional amount of methanol was added and the reaction was allowed to reflux for an additional 30 min to yield a light orange solid. This was then vacuum filtered and washed with Methanol. The resulting white power was recrystallized in a 1:2 Methanol and Ethyl Acetate mixture, hot filtered and allowed to cool to room temp to afford a white crystalline material. Yield(.915g, 49%). MP: 210-212°C. H¹ NMR (d₆ DMSO, 300MHz): δ =2.71 (s, 3H), δ 4.54 (d 1H) δ 4.56 (d, 1H) δ 4.68 (s,2H) δ 4.69 (s,2H) δ 7.25 (d,2H), δ 7.63 (ddd,1H), δ 8.50, (ddd,2H) ppm. C¹³ NMR (CDCl₃ or d₆ DMSO, 300MHz): δ 173, δ 150, δ 148, δ 123, δ 73 ppm. FTIR (ATR): 3295, 1650, 1596, 1569, 1479, 1443, 1425, 1409, 1357, 1328, 1285, 1254, 1217, 1144, 1082, 1023, 1052.

3-Pyridyl Tartaramide and Fumaric acid Fumaric acid (.9847g, 2.9mol), 3-Pyridyl Tartaramide (.346g, 2.9 mol) was added to a flask containing methanol (50 ml). The reaction was stirred and heated until it dissolved. The solution was hot filtered into siled glassware and allowed to recrystallize. Percent Yield: (1.009g, 90%). MP: ^1H NMR (d_6 DMSO, 300MHz): $\delta=8.4$ (m, 6H), δ 7.6 (d, 2H), δ 7.3, (m,2H) δ (s,2H), δ 4.3(m, 6H). FTIR (ATR): 3372, 1775, 1697, 1642, 1604, 1593, 1534, 1431, 1358, 1315, 1263, 1227, 1201, 1182, 1120, 1082, 1051, 971, 895, 837, 837, 837, 782, 703 cm^{-1} . ^{13}C NMR: $\delta=$ 172, δ 168, δ 149, δ 148, δ 124, δ 74 ppm.

(2E)-3-phenylprop-2-enal³⁶ Vinyl Acetate (1.1ml, 12mmol) and Benzaldehyde (1.0ml, 10mmol) in THF (10ml) was added drop wise to a stirring solution of $\text{Ba}(\text{OH})_2 \cdot 8(\text{H}_2\text{O})$ (3.6g, 12mmol) in THF (20ml). The reaction mixture refluxed for 10 hours, or until all the benzaldehyde was used up as indicated by TLC. The reaction was then poured into cold water and filtered to remove Barium salt. The filtrate was extracted with chloroform, and the organic layer was washed with water, dried with magnesium sulfate and evaporated to yield a crude aldehyde, purified by column chromatography(silica gel) eluting with hexane to afford the pure cinnamaldehyde (.6857ml, 95 %) ^1H NMR (d_6 DMSO, 300MHz): $\delta=9.4$ (d, 1H), δ 7.6 (d,1H), δ 7.5 (m, 1H), δ 7.46 (t,1H), δ 7.4, (m, 1H) δ 6.6 (dd, 1H).

Cinnamylidene Malonic acid³⁷ Cinnamaldehyde (1ml, .0075mol), Malonic acid (.8033g, .0075mol), and Pyridine (.1ml, .0011mol) was added to a reaction vessel. The solution was refluxed under argon until the internal temperature reached 80°C. The temperature remained at 80°C for 30 minutes. The reaction was cooled to room

temperature to afford a white precipitate. The precipitate was crushed and dissolved in 20ml of aqueous Na_2CO_3 (10%). It was then extracted with diethyl ether to remove unreacted cinnamaldehyde. The solution containing the aqueous Na_2CO_3 was acidified with a (1:1) HCL/ H_2O solution. This produced a yellow solid which was then filtered out, washed with distilled H_2O , followed by hot benzene to remove cinnamylidene acetic acid. The precipitate was dried and recrystallized from ethanol. Crystals should resemble yellow needles. Yield: (.78g, 58%). MP: 208-210°C. H NMR: δ 7.47(1H, dddd), δ 7.49 (dddd, 1H), δ 7.53 (1H, dddd), δ 7.74 (tt, 1H), δ 7.80 (d,1H), δ 8.38 (d,1H)ppm. C^{13} : δ 167, δ 166, δ 144, δ 143, δ 136, δ 130, δ 129, δ 128, δ 127, δ 123. FTIR (ATR): 2453, 1709, 1638, 1601, 1573, 1558, 1425, 1491, 1365, 1311, 1271, 1218, 1172, 1062, 1024, 996, 987, 945, 862, 807, 752, 714 cm^{-1} .

UV Study Using FTIR/ATR and Polymorph 1: The experiment consisted of preparing a BaF_2 and Cinnamylidene Malonic acid into a pellet and placing it into the UV photoreactor (253.7 A) for various time intervals. The average temperature within the box was 23.7C. It was then placed in the FTIR/ATR for analysis. This procedure was repeated several times over a period of approximately 400 minutes at 10-20 minute intervals

UV Study Using H^1NMR and Polymorph 2: The experiment consisted of placing Cinnamylidene Malonic acid (.8980g) in a quartz round bottom containing 75ml of Hexanes. The solution was placed into the photoreactor (253.7 A). The temperature inside the photoreactor averaged 41C with a median and mode of 42C. The samples collected at 10-20 minutes intervals over a period of 600 minutes. Samples collected were

vacuum filtered while the solution containing the crystals was placed in a 40C water bath to maintain temperature. It was also protected against ambient light by covering with aluminum foil. The samples were placed in NMR tubes and placed in a container covered with foil. The reaction progress was followed using H^1 NMR: Monomer δ 7.8 (m, 10H). Dimer δ 6.8 (2H, d), δ 4.2 (2H,d).

REFERENCES

- ¹Matsumoto, A., Tanaka, T., Kohji, T., Saragai, S., Nakamotot,S, S; *J.AM. CHEM. SOC.* **2002**, Vol. 124, 8891-8902
- ²Matsumoto, A.; Yokoi, K.; Aoki, S.; Tashiro, K., Kamae., Kobayashi, M. *Macromolecules* **1998**,Vol. 31, 2129-2136
- ³Gonzalez, S, Carlson, P; *Tetrahedron Letters* Vol. 49. **2008**, 3925-3926.
- ⁴Saragai,S., Tashiro,K., Nakamotot,S., Matsumoto, A., Tsubouchi,T; *J. Phys. Chem. B* **2001**, 105,4155-4165.
- ⁵[http:// www.ccdc.cam.ac.uk/products/csd](http://www.ccdc.cam.ac.uk/products/csd)
- ⁶ Julian, M.; *Foundations in Crystallography with Computer Applications.* **2008**.
- ⁷D, Craig., Desiraju, G ; *J. Am. Chem. Soc.* **1996**, Vol. 118, 4090-4093.
- ⁸MacGillivray, L., Papaefstathiou, G; *Encyclopedia of Supramolecular Chemistry*, **2004**.
- ⁹ Matsumotot, A., A., Furukawa, D., and Nakazawa, H; *J. Poly. Science.* Vol. 44,4952-4965, **2006**.
- ¹⁰ “The Choice of Pharmaceutical Crystalline Form can be used to Optimize Drug Properties, and Co-crystals are emerging as New Alternatives”.
[http:// www.Pubs.acs.org](http://www.Pubs.acs.org).
- ¹¹ Schmidt, G., J, Cohen, MD; *J. Chem. Soc.* **1964**
- ¹²Masaaki,T., Yamashita, Y; *CrystEngComm*, **2000**. Vol 16.
- ¹³Jiao, P, Chan, C; *Tetrahedron: Asymmetry.* Vol. 12. **2001**, 3081-3088.
- ¹⁴ Ren, C., Bao, Y., Chen, L; *CrystEngComm*, **2004**, Vol. 6(35), 200-206.
- ¹⁵ Cohen, M. D.; Schmidt, G. M. J.; Sonntag, F. I. *J. Chem. Soc.* **1964**
- ¹⁶“Propylene Tacticity”. <http://www.chem.rochester.edu>.
- ¹⁷Matsumoto, A., Tanaka, T., Oka, K; *Synthesis* **2005**, No 9, 1479- 1490
- ¹⁸Houston, T. Wilkenson, B; *Organic Letters.* **2004** Vol.6, No.5. Pg 679-681.
- ¹⁹Chen, W. Lui, Y; *J. Org. Chem.* **2005**, Pg 1665-1668.

- ²⁰ Mahata, M. Prenab, K. Okram, Barun, H; *Synlet*. **2000**, No.9, Pg 1345-1347.
- ²¹ Hoogen, N., Oskar, N; *J. Polymer Science. Part A: Polymer Chemistry*, Vol. 38, **2000**. Pg 1903-1910.
- ²² Matsumoto, A., Odani, T., Chikada, M., Sada, K., Miyata, M. *J. Am. Chem. Soc.* **1999**, Vol. *121*, 11122-11129.
- ²³ R. K. McMullan., W. T. Klooster., H; *Acta Cryst.* **2008**. B64, 230-239.
- ²⁴ Jeffrey, G. *An Introduction to Hydrogen Bonding*. New York. Oxford Press. **1997**.
- ²⁵ Coates, G., Dunn, A., Henling, L., Ziller, J., Lobkovsky., Grubbs, R. *J. Am. Chem. Soc.* **1998**, 120, 3641-3649.
- ²⁶ Boyle, P.D. Growing Crystals That Will Make Your Crystallographer Happy.
<http://www.xray.ncsu.edu/GrowXtal.html> (accessed Jul 2009).
- ²⁷ Matsumoto, A; *Progress in Reaction Kinetics and Mechanism*. **2001**, Vol. 26, 1468-6783.
- ²⁸ Moulton, B., Zaworotko; *J. Chem. Rev.* **2001**, Vol. 101, 1629- 1658.
- ²⁹ Massicot, F., Plantier, C., Portella, D., Saleur, A. Sudha, R; *Synthesis* 2001.No 16,30 11 **2001**.
- ³⁰ Gnanaguru, K., Ramasubbu, N., Venkatesan, K., and Ramamurthy, V; *J. Org. Chem* , **1985**, 50, 2337-2346.
- ³¹ Montanuado, G., and Caccamese, S; *J. Org. Chem*, Vol.38, No. 4, **1973**.
- ³² Zumdahl, S., Zumdahl, S. *Zumdahl Chemistry* 5th Ed. Houghton McMillan. **2000**.
- ³³ West, A. *Basic Solid State Chemistry*. John Wiley and Sons. **1989**.
- ³⁴ Houston, T. Wilkenson, B. *Organic Letters*. 2004 Vol.6, No.5. Pg 679-681.
- ³⁵ Chen, W. Lui, Y. *J. Org. Chem.* 2005, 1665-1668.
- ³⁶ Mahata, M. Prenab, K. Okram, Barun, H. *Synlet* 2000, No.9, 1345-1347.
- ³⁷ Hoogen, N, Oskar, N. *J. Poly. Science. Part A: Polymer Chemistry*. Vol. 38, 2000. 1903-1910.
- ³⁸ Turowska, I., *J. Phys. Org. Chem.* **2004**; 17: 837-847.

Appendix 1. Crystallographic Data

Crystal structures were obtained by Dr. Robert Pike and James S. Jones at the University of William and Mary. Crystals were mounted on glass fibers. All measurements were made using graphite-monochromated CuK α radiation on a Bruker-AXS three-circle diffractometer, equipped with a SMART Apex II CCD detector. The data were reduced using SAINT+ⁱ, and empirical or numerical absorption correction applied using SADABSⁱⁱ. Structures were solved using direct methods. Least squares refinement for all structures was carried out on F². The non-hydrogen atoms were refined anisotropically. Hydrogen atoms that could be located in the Fourier difference map were refined isotropically; the remaining hydrogen's were refined isotropically as riding models. Structure solution, refinement and the calculation of derived results were performed using the SHELXTL package of computer programsⁱⁱⁱ. Packing diagrams were produced using Mercury^{iv}. The absolute configuration was determined using the method of Flack et.al.^v

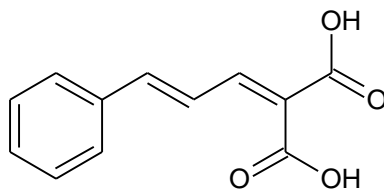


Table 6. Selected Crystal data and refinement parameters for (E,E)-Cinnamylidenemalonic acid

Empirical formula	$C_{12}H_{10}O_4$	
Formula weight	218.20	
Temperature	100(2) K	
Crystal system	Monoclinic	
Space group	$P2(1)/c$	
Unit cell dimensions	$a = 6.9763(2) \text{ \AA}$	$\beta = 90^\circ$.
	$b = 10.4935(2) \text{ \AA}$	$\gamma = 96.9330(10)^\circ$.
	$c = 13.8570(3) \text{ \AA}$	$\alpha = 90^\circ$.
Volume	$1007.00(4) \text{ \AA}^3$	
Z	4	
Density (calculated)	1.439 mg/mm^3	
Absorption coefficient	0.914 mm^{-1}	
Index ranges	$-8 \leq h \leq 7, -11 \leq k \leq 12, -16 \leq l \leq 16$	
Reflections collected	10441	
Independent reflections	1717 [R(int) = 0.0344]	
Completeness to $\theta = 66.97^\circ$	95.4 %	
Data / restraints / parameters	1717 / 0 / 153	
Goodness-of-fit on F^2	1.207	
Final R indices [I > 2 σ (I)]	R1 = 0.0573, wR2 = 0.1490	
R indices (all data) hole	R1 = 0.0586, wR2 = 0.1495 Largest diff. peak and hole	0.335 and $-0.344 \text{ e.\AA}^{-3}$

ORTEP diagram and atom labeling scheme

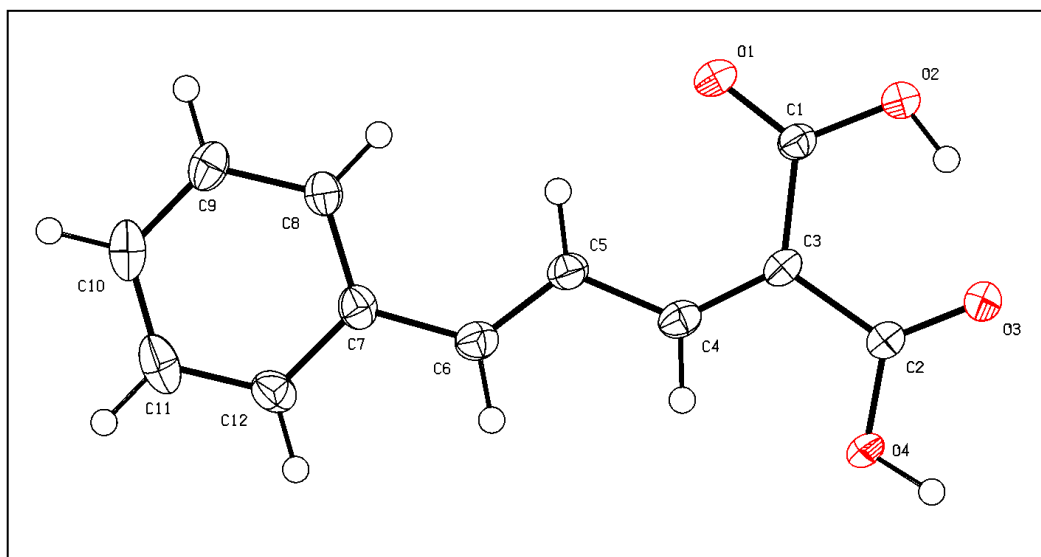


Table 7. Atomic coordinates ($\times 10^4$) and equivalent isotropic displacement parameters ($\text{\AA}^2 \times 10^3$). $U(\text{eq})$ is defined as one third of the trace of the orthogonalized U^{ij} tensor.

	x	y	z	$U(\text{eq})$
O(1)	1872(4)	12845(2)	5235(2)	32(1)
O(2)	1377(3)	14273(2)	4068(2)	29(1)
O(3)	1029(3)	13531(2)	2300(1)	25(1)
O(4)	1170(3)	11451(2)	1973(1)	27(1)
C(1)	1611(4)	13086(3)	4368(2)	21(1)
C(2)	1224(4)	12418(3)	2581(2)	20(1)
C(3)	1568(4)	12061(3)	3623(2)	21(1)
C(4)	1849(4)	10813(3)	3850(2)	22(1)
C(5)	2322(4)	10214(3)	4776(2)	23(1)
C(6)	2513(4)	8934(3)	4823(2)	25(1)
C(7)	3031(4)	8175(3)	5693(2)	24(1)

C(8)	3257(4)	8701(3)	6625(2)	24(1)
C(9)	3786(4)	7936(3)	7430(2)	28(1)
C(10)	4082(5)	6649(3)	7323(3)	33(1)
C(11)	3832(5)	6103(3)	6402(3)	36(1)
C(12)	3318(5)	6861(3)	5600(2)	28(1)

Table 8. Anisotropic displacement parameters ($\text{\AA}^2 \times 10^{-3}$) for p21onc. The anisotropic displacement factor exponent takes the form: $-2 \sum [h^2 a^{*2} U^{11} + \dots + 2 h k a^* b^* U^{12}]$

	U ¹¹	U ²²	U ³³	U ²³	U ¹³	U ¹²
O(1)	51(2)	29(1)	17(1)	-2(1)	5(1)	4(1)
O(2)	45(1)	22(1)	20(1)	-1(1)	2(1)	4(1)
O(3)	32(1)	23(1)	20(1)	2(1)	3(1)	2(1)
O(4)	45(1)	23(1)	13(1)	0(1)	5(1)	-1(1)
C(1)	23(2)	23(2)	18(1)	-1(1)	3(1)	1(1)
C(2)	19(1)	24(2)	18(1)	0(1)	2(1)	0(1)
C(3)	21(1)	25(2)	15(1)	0(1)	2(1)	-1(1)
C(4)	21(1)	27(2)	19(1)	-2(1)	4(1)	-3(1)
C(5)	27(2)	24(2)	19(1)	-2(1)	2(1)	-3(1)
C(6)	26(2)	27(2)	22(2)	-2(1)	5(1)	-1(1)
C(7)	23(2)	22(2)	27(2)	4(1)	7(1)	-3(1)
C(8)	25(2)	22(2)	26(2)	4(1)	4(1)	-2(1)
C(9)	27(2)	34(2)	24(2)	7(1)	5(1)	-3(1)
C(10)	28(2)	33(2)	40(2)	17(2)	5(2)	4(1)
C(11)	32(2)	25(2)	52(2)	12(2)	14(2)	4(1)
C(12)	31(2)	22(2)	31(2)	-2(1)	12(1)	-2(1)

Table9. Hydrogen bonds for p21onc [\AA and deg].

D-H...A	d(D-H)	d(H...A)	d(D...A)	<(DHA)
O(4)-H(4O)...O(1)#1	0.94(4)	1.70(4)	2.620(3)	164(4)
O(2)-H(2O)...O(3)	0.87(3)	1.73(4)	2.554(3)	157(3)

Symmetry transformations used to generate equivalent atoms:

#1 $x, -y+5/2, z-1/2$

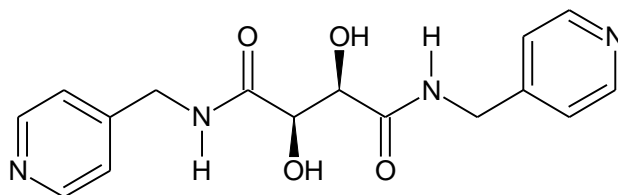


Table 10. Selected Crystal data and refinement parameters (2R, 3R)-2,3-dihydroxy-N,N'-bis(pyridine-4-ylmethyl) butanediamide.

Empirical formula	$C_{16}H_{18}N_4O_4$	
Formula weight	330.34	
Temperature	100(2) K	
Crystal system	Monoclinic	
Space group	C2	
Unit cell dimensions	$a = 20.3768(4) \text{ \AA}$	$\alpha = 90^\circ$.
	$b = 5.16640(10) \text{ \AA}$	$\beta = 107.3100(10)^\circ$.
	$c = 14.9581(3) \text{ \AA}$	$\gamma = 90^\circ$.
Volume	$1503.39(5) \text{ \AA}^3$	
Z	4	
Density (calculated)	1.460 mg/mm^3	
Absorption coefficient	0.893 mm^{-1}	
Index ranges	$-24 \leq h \leq 23, -6 \leq k \leq 5, -17 \leq l \leq 17$	
Reflections collected	7747	
Independent reflections	2343 [R(int) = 0.0308]	
Data / restraints / parameters	2343 / 1 / 289	
Goodness-of-fit on F^2	1.046	
Final R indices [I > 2 σ (I)]	R1 = 0.0271, wR2 = 0.0732	
R indices (all data)	R1 = 0.0283, wR2 = 0.0749	
Largest diff. peak and hole	0.147 and $-0.164 \text{ e.\AA}^{-3}$	

ORTEP diagram with atom labeling scheme

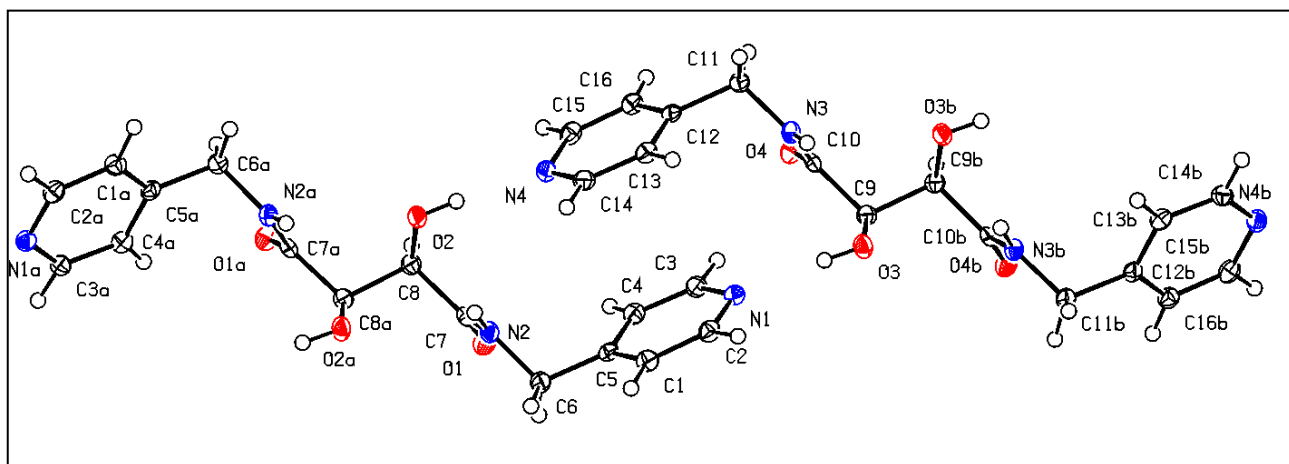


Table 11. Atomic coordinates ($\times 10^4$) and equivalent isotropic displacement parameters ($\text{\AA}^2 \times 10^3$) for c2. $U(\text{eq})$ is defined as one third of the trace of the orthogonalized U^{ij} tensor.

	x	y	z	$U(\text{eq})$
O(1)	656(1)	-1681(2)	6666(1)	21(1)
O(2)	654(1)	2915(2)	4903(1)	21(1)
N(1)	2947(1)	4188(3)	9105(1)	19(1)
N(2)	633(1)	2702(3)	6737(1)	16(1)
C(1)	1768(1)	5494(4)	8792(1)	19(1)
C(2)	2470(1)	5839(3)	9206(1)	19(1)
C(3)	2723(1)	2105(3)	8560(1)	19(1)
C(4)	2037(1)	1628(3)	8115(1)	19(1)
C(5)	1542(1)	3339(3)	8232(1)	16(1)
C(6)	785(1)	2866(3)	7754(1)	18(1)
C(7)	577(1)	467(3)	6279(1)	16(1)
C(8)	395(1)	670(3)	5212(1)	17(1)
O(3)	4332(1)	4898(2)	10080(1)	21(1)
O(4)	4387(1)	397(2)	8312(1)	21(1)

N(3)	4359(1)	4773(3)	8249(1)	16(1)
N(4)	2030(1)	3483(3)	5904(1)	20(1)
C(9)	4608(1)	2681(3)	9776(1)	16(1)
C(10)	4443(1)	2529(3)	8708(1)	15(1)
C(11)	4192(1)	4855(3)	7234(1)	17(1)
C(12)	3434(1)	4360(3)	6764(1)	16(1)
C(13)	2937(1)	6050(3)	6894(1)	18(1)
C(14)	2249(1)	5555(4)	6455(1)	20(1)
C(15)	2510(1)	1872(3)	5784(1)	20(1)
C(16)	3209(1)	2225(3)	6194(1)	19(1)

Table 12. Anisotropic displacement parameters ($\text{\AA}^2 \times 10^3$). The anisotropic displacement factor exponent takes the form: $-2p^2[h^2 a^* 2U^{11} + \dots + 2 h k a^* b^* U^{12}]$

	U ¹¹	U ²²	U ³³	U ²³	U ¹³	U ¹²
O(1)	24(1)	16(1)	20(1)	2(1)	5(1)	2(1)
O(2)	16(1)	28(1)	19(1)	4(1)	2(1)	-6(1)
N(1)	18(1)	22(1)	17(1)	1(1)	5(1)	-2(1)
N(2)	15(1)	16(1)	16(1)	2(1)	2(1)	0(1)
C(1)	20(1)	18(1)	19(1)	1(1)	7(1)	2(1)
C(2)	23(1)	18(1)	17(1)	-1(1)	5(1)	-3(1)
C(3)	18(1)	20(1)	18(1)	0(1)	6(1)	3(1)
C(4)	21(1)	18(1)	18(1)	0(1)	6(1)	-2(1)
C(5)	19(1)	18(1)	13(1)	3(1)	5(1)	0(1)
C(6)	17(1)	20(1)	17(1)	-2(1)	5(1)	1(1)
C(7)	10(1)	18(1)	19(1)	0(1)	4(1)	0(1)
C(8)	16(1)	17(1)	18(1)	1(1)	5(1)	2(1)

O(3)	15(1)	25(1)	20(1)	-6(1)	2(1)	3(1)
O(4)	25(1)	17(1)	18(1)	-2(1)	4(1)	1(1)
N(3)	16(1)	14(1)	16(1)	-2(1)	2(1)	-1(1)
N(4)	17(1)	24(1)	17(1)	3(1)	4(1)	-2(1)
C(9)	17(1)	16(1)	17(1)	-2(1)	5(1)	-2(1)
C(10)	9(1)	18(1)	17(1)	0(1)	3(1)	-1(1)
C(11)	17(1)	17(1)	16(1)	3(1)	4(1)	-1(1)
C(12)	17(1)	17(1)	13(1)	4(1)	4(1)	-2(1)
C(13)	22(1)	15(1)	17(1)	-1(1)	6(1)	-1(1)
C(14)	19(1)	22(1)	19(1)	2(1)	7(1)	2(1)
C(15)	25(1)	17(1)	17(1)	0(1)	5(1)	-2(1)
C(16)	21(1)	18(1)	17(1)	1(1)	6(1)	1(1)

Table 13. Hydrogen bonds for c2 [\AA and $^\circ$].

D-H...A	d(D-H)	d(H...A)	d(D...A)	$\angle(\text{DHA})$
N(2)-H(2N)...O(1)#3	0.88(2)	2.16(2)	2.9052(19)	142.1(16)
O(2)-H(2O)...N(4)	0.856(19)	1.919(19)	2.7733(15)	176(2)
N(3)-H(3N)...O(4)#3	0.88(2)	2.18(3)	2.9070(19)	140.1(16)
O(3)-H(3O)...N(1)	0.84(2)	1.96(2)	2.7876(16)	170(2)

Symmetry transformations used to generate equivalent atoms:

#1 -x,y,-z+1 #2 -x+1,y,-z+2 #3 x,y+1,z

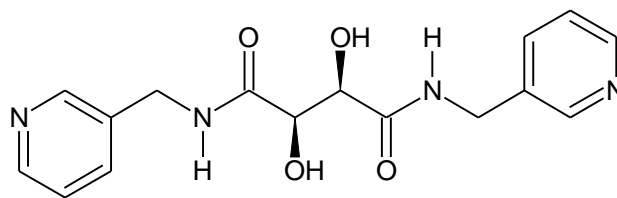


Table 14. Crystal data and structure refinement for (2R, 3R)-2,3-dihydroxy-N,N'-bis(pyridine-3-ylmethyl) butanediamide

Empirical formula	C ₁₆ H ₁₈ N ₄ O ₄
Formula weight	330.34
Temperature	296(2) K
Crystal system	Orthorhombic
Space group	P2(1)2(1)2(1)
Unit cell dimensions	a = 5.09760(10) Å α = 90° b = 17.3073(3) Å β = 90° c = 17.8192(3) Å γ = 90°
Volume	1572.11(5) Å ³
Calculated density	1.396 mg/mm ³
Z	4
Absorption coefficient	0.854 mm ⁻¹
Index range	-5 ≤ h ≤ 6, -20 ≤ k ≤ 20, -19 ≤ l ≤ 21
Reflections collected	16977
Independent reflections	2735 [R(int) = 0.0277]
Data / restraints / parameters	2735 / 0 / 290
Goodness-of-fit on F ²	1.025
Final R indices [I > 2σ(I)]	R1 = 0.0236, wR2 = 0.0685
R indices (all data)	R1 = 0.0237, wR2 = 0.0686
Extinction coefficient	0.0081(6)
Largest diff. peak and hole	0.126 and -0.100 e.Å ⁻³

ORTEP diagram with atom labeling scheme

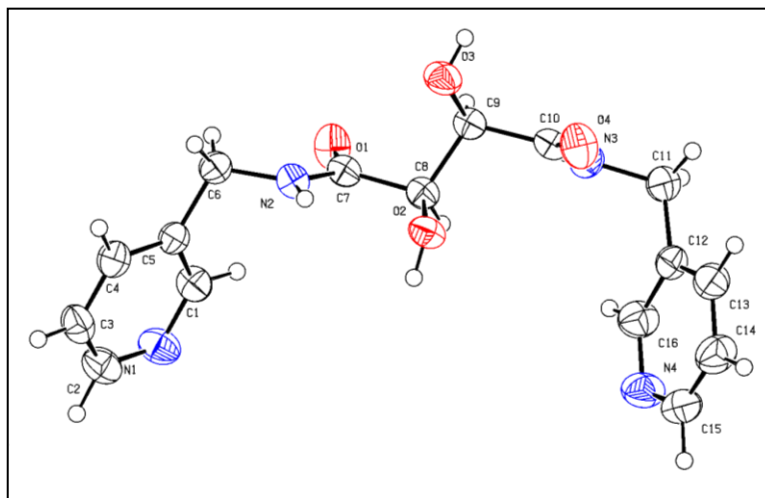


Table 15 Atomic coordinates ($\times 10^4$) and equivalent isotropic displacement parameters ($\text{\AA}^2 \times 10^3$). U(eq) is defined as one third of the trace of the orthogonalized Uij tensor.

	x	y	z	U(eq)
O(1)	5646(2)	-210(1)	1318(1)	50(1)
O(2)	10476(2)	1291(1)	1370(1)	41(1)
O(3)	8468(2)	857(1)	2782(1)	48(1)
O(4)	8342(2)	2458(1)	2613(1)	53(1)
N(1)	9729(2)	-1126(1)	-942(1)	50(1)
N(2)	10068(2)	-264(1)	1319(1)	35(1)
N(3)	4394(2)	2369(1)	2043(1)	40(1)
N(4)	6467(3)	3781(1)	152(1)	56(1)
C(1)	9310(3)	-991(1)	-212(1)	42(1)
C(2)	11863(3)	-1538(1)	-1120(1)	49(1)
C(3)	13566(3)	-1822(1)	-597(1)	47(1)
C(4)	13095(3)	-1683(1)	156(1)	42(1)
C(5)	10915(2)	-1255(1)	359(1)	34(1)
C(6)	10243(3)	-1089(1)	1170(1)	38(1)
C(7)	7798(2)	107(1)	1366(1)	34(1)
C(8)	7924(2)	986(1)	1464(1)	34(1)
C(9)	6838(2)	1189(1)	2237(1)	34(1)
C(10)	6621(2)	2069(1)	2321(1)	36(1)
C(11)	3934(3)	3200(1)	2055(1)	47(1)
C(12)	5486(3)	3617(1)	1460(1)	40(1)
C(13)	7284(3)	4182(1)	1631(1)	49(1)
C(14)	8692(4)	4536(1)	1062(1)	57(1)
C(15)	8213(3)	4323(1)	338(1)	53(1)
C(16)	5157(3)	3439(1)	708(1)	51(1)

Table 16. Anisotropic displacement parameters ($\text{\AA}^2 \times 10^3$). The anisotropic displacement factor exponent takes the form: $-2p^2[h^2 a^* 2 U^{11} + \dots + 2 h k a^* b^* U^{12}]$

	U11	U22	U33	U23	U13	U12
O(1)	29(1)	48(1)	73(1)	-10(1)	-3(1)	-2(1)
O(2)	39(1)	48(1)	34(1)	-5(1)	5(1)	-8(1)
O(3)	54(1)	59(1)	31(1)	3(1)	-2(1)	16(1)
O(4)	46(1)	53(1)	60(1)	-15(1)	-10(1)	-4(1)
N(1)	45(1)	67(1)	37(1)	-2(1)	-4(1)	1(1)
N(2)	28(1)	39(1)	38(1)	-4(1)	-2(1)	-1(1)
N(3)	37(1)	40(1)	44(1)	3(1)	-1(1)	1(1)
N(4)	68(1)	64(1)	36(1)	2(1)	-4(1)	-5(1)
C(1)	36(1)	48(1)	40(1)	-1(1)	-4(1)	5(1)
C(2)	47(1)	59(1)	40(1)	-9(1)	2(1)	-6(1)
C(3)	43(1)	47(1)	52(1)	-9(1)	8(1)	2(1)
C(4)	40(1)	39(1)	47(1)	1(1)	-3(1)	3(1)
C(5)	33(1)	32(1)	36(1)	0(1)	-2(1)	-2(1)
C(6)	40(1)	38(1)	35(1)	2(1)	-2(1)	4(1)
C(7)	30(1)	42(1)	31(1)	-2(1)	-3(1)	-1(1)
C(8)	32(1)	40(1)	31(1)	-2(1)	-4(1)	0(1)
C(9)	31(1)	39(1)	33(1)	0(1)	-1(1)	1(1)
C(10)	34(1)	43(1)	30(1)	-3(1)	3(1)	-1(1)
C(11)	49(1)	44(1)	48(1)	4(1)	9(1)	9(1)
C(12)	43(1)	37(1)	40(1)	2(1)	-1(1)	7(1)
C(13)	67(1)	44(1)	38(1)	-2(1)	-7(1)	-1(1)
C(14)	67(1)	49(1)	55(1)	4(1)	-6(1)	-12(1)
C(15)	58(1)	53(1)	47(1)	10(1)	4(1)	-3(1)
C(16)	56(1)	55(1)	43(1)	0(1)	-6(1)	-8(1)

Table 17. Hydrogen bonds for p2(1)2(1)2(1) [A and deg.].

D-H...A	d(D-H)	d(H...A)	d(D...A)	<(DHA)
O(3)-H(3O)...N(1)#1	0.839(19)	2.01(2)	2.8361(14)	168.8(18)
O(2)-H(2O)...N(4)#2	0.87(2)	1.89(2)	2.7602(15)	172(2)
N(3)-H(3N)...O(2)#3	0.91(2)	2.09(2)	2.9846(15)	169.8(17)
N(2)-H(2N)...O(1)#4	0.891(17)	2.109(17)	2.8454(14)	139.4(12)

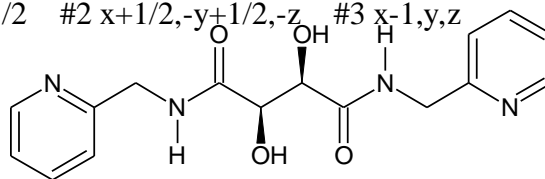
Symmetry transformations used to generate equivalent atoms:

#1 $-x+3/2, -y, z+1/2$

#2 $x+1/2, -y+1/2, -z$

#3 $x-1, y, z$

#4 $x+1, y, z$

**Table 18.** Selected Crystal data and refinement parameters (2R, 3R)-2,3-dihydroxy-N,N'-bis(pyridine-3-ylmethyl) butanediamide

Empirical formula	C ₁₆ H ₂₂ N ₄ O ₆	
Formula weight	366.38	
Temperature	100(2) K	
Crystal system	Orthorhombic	
Space group	P2(1)2(1)2(1)	
Unit cell dimensions	a = 4.98690(10) Å	a = 90°.
	b = 9.05490(10) Å	b = 90°.
	c = 38.9812(6) Å	g = 90°.
Volume	1760.23(5) Å ³	
Z	4	
Density (calculated)	1.383 mg/mm ³	

Absorption coefficient	0.902 mm ⁻¹
Reflections collected	19094
Independent reflections	3057 [R(int) = 0.0252]
Completeness to theta = 66.94°	99.5 %
Data / restraints / parameters	3057 / 0 / 323
Goodness-of-fit on F ²	1.068
Final R indices [I>2sigma(I)]	R1 = 0.0282, wR2 = 0.0777
R indices (all data)	R1 = 0.0282, wR2 = 0.0777
Largest diff. peak and hole	0.176 and -0.236 e.Å ⁻³

ORTEP diagram and atom labeling scheme

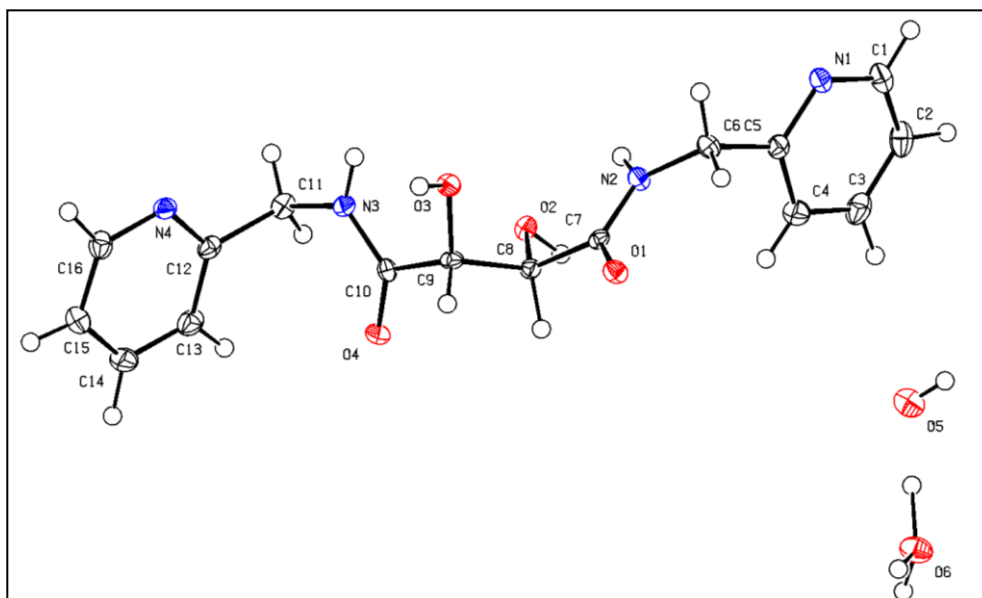


Table 19. Atomic coordinates ($\times 10^4$) and equivalent isotropic displacement parameters ($\text{\AA}^2 \times 10^3$) $U(\text{eq})$ is defined as one third of the trace of the orthogonalized U^{ij} tensor.

	x	y	z	$U(\text{eq})$
O(1)	5239(2)	7684(1)	6388(1)	16(1)
O(2)	-310(2)	6575(1)	6915(1)	14(1)
O(3)	3092(2)	9229(1)	7085(1)	15(1)
O(4)	2966(2)	5851(1)	7572(1)	18(1)
N(1)	-2524(3)	8369(2)	5535(1)	16(1)
N(2)	743(3)	7900(1)	6329(1)	15(1)
N(3)	868(3)	8055(1)	7639(1)	15(1)
N(4)	2051(3)	8946(1)	8381(1)	15(1)
C(1)	-4119(3)	7591(2)	5322(1)	21(1)
C(2)	-4176(4)	6079(2)	5309(1)	24(1)
C(3)	-2409(4)	5303(2)	5517(1)	24(1)
C(4)	-732(4)	6080(2)	5734(1)	22(1)

C(5)	-871(3)	7616(2)	5741(1)	15(1)
C(6)	810(3)	8514(2)	5986(1)	16(1)
C(7)	2946(3)	7517(2)	6500(1)	12(1)
C(8)	2445(3)	6780(2)	6849(1)	13(1)
C(9)	3685(3)	7709(2)	7139(1)	13(1)
C(10)	2488(3)	7125(2)	7473(1)	14(1)
C(11)	-534(3)	7606(2)	7952(1)	17(1)
C(12)	1341(3)	7614(2)	8258(1)	16(1)
C(13)	2301(4)	6307(2)	8395(1)	22(1)
C(14)	4102(4)	6365(2)	8667(1)	25(1)
C(15)	4859(3)	7733(2)	8795(1)	23(1)
C(16)	3782(4)	8983(2)	8645(1)	20(1)
O(5)	2395(2)	2660(1)	5360(1)	27(1)
O(6)	7380(3)	1311(1)	5332(1)	25(1)

Table 20. Anisotropic displacement parameters ($\text{\AA}^2 \times 10^3$). The anisotropic displacement factor exponent takes the form: $-2p^2[h^2 a^{*2} U^{11} + \dots + 2 h k a^* b^* U^{12}]$

	U ¹¹	U ²²	U ³³	U ²³	U ¹³	U ¹²
O(1)	12(1)	20(1)	17(1)	2(1)	1(1)	1(1)
O(2)	13(1)	15(1)	15(1)	-2(1)	1(1)	-2(1)
O(3)	17(1)	11(1)	18(1)	0(1)	-3(1)	-2(1)
O(4)	22(1)	14(1)	18(1)	3(1)	-2(1)	4(1)
N(1)	16(1)	20(1)	14(1)	2(1)	-1(1)	0(1)
N(2)	11(1)	20(1)	13(1)	2(1)	1(1)	0(1)
N(3)	19(1)	12(1)	14(1)	-1(1)	0(1)	2(1)
N(4)	18(1)	13(1)	16(1)	1(1)	2(1)	2(1)

C(1)	20(1)	29(1)	16(1)	2(1)	-3(1)	-2(1)
C(2)	28(1)	27(1)	17(1)	-2(1)	1(1)	-11(1)
C(3)	32(1)	19(1)	21(1)	-5(1)	3(1)	-5(1)
C(4)	24(1)	20(1)	21(1)	1(1)	0(1)	2(1)
C(5)	13(1)	19(1)	13(1)	1(1)	3(1)	0(1)
C(6)	14(1)	17(1)	16(1)	2(1)	-2(1)	-2(1)
C(7)	12(1)	9(1)	15(1)	-3(1)	0(1)	0(1)
C(8)	11(1)	14(1)	13(1)	-1(1)	-1(1)	1(1)
C(9)	13(1)	9(1)	17(1)	-1(1)	-1(1)	1(1)
C(10)	12(1)	16(1)	13(1)	-2(1)	-4(1)	-2(1)
C(11)	17(1)	17(1)	18(1)	-1(1)	2(1)	-2(1)
C(12)	18(1)	14(1)	15(1)	1(1)	6(1)	0(1)
C(13)	32(1)	14(1)	20(1)	1(1)	6(1)	1(1)
C(14)	35(1)	18(1)	22(1)	5(1)	1(1)	7(1)
C(15)	26(1)	24(1)	17(1)	3(1)	-2(1)	3(1)
C(16)	24(1)	19(1)	16(1)	0(1)	1(1)	-3(1)
O(5)	25(1)	27(1)	28(1)	3(1)	-3(1)	1(1)
O(6)	26(1)	19(1)	31(1)	6(1)	-2(1)	1(1)

Table 21. Hydrogen bonds for p212121 [\AA and deg].

D-H...A	d(D-H)	d(H...A)	d(D...A)	\angle (DHA)
N(2)-H(2N)...O(1)#1	0.89(2)	1.97(2)	2.7613(18)	147.8(17)
N(2)-H(2N)...O(2)	0.89(2)	2.201(19)	2.6326(16)	109.5(16)
O(2)-H(2O)...N(4)#2	0.95(3)	1.84(3)	2.7848(16)	175(3)
N(3)-H(3N)...O(4)#3	0.95(2)	2.44(2)	3.2774(17)	146.7(17)
O(3)-H(3O)...O(4)#4	0.81(3)	1.99(2)	2.7955(16)	175(2)
O(5)-H(1W)...O(6)#5	0.78(2)	2.09(2)	2.8567(18)	168(2)

O(6)-H(2W)...O(5)	1.26(6)	1.52(6)	2.7720(18)	173(5)
O(6)-H(3W)...N(1)#6	0.93(3)	1.87(3)	2.7788(17)	166(3)
O(6)-H(4W)...O(5)#7	1.22(5)	1.57(5)	2.7851(18)	175(4)

Symmetry transformations used to generate equivalent atoms:

#1 $x-1, y, z$ #2 $-x, y-1/2, -z+3/2$ #3 $-x, y+1/2, -z+3/2$

#4 $-x+1, y+1/2, -z+3/2$ #5 $x-1/2, -y+1/2, -z+1$ #6 $x+1, y-1, z$

#7 $x+1, y, z$

ⁱ SAINT PLUS (2001) Bruker analytical X-ray systems. Madison,

WI

ⁱⁱ SADABS (2001) Bruker analytical X-ray systems. Madison, WI

ⁱⁱⁱ Sheldrick GM (2008) *Acta Crystallogr Sect A* 64:112

^{iv} Mercury 1.4.2 (2007) Cambridge crystallographic data centre.

Cambridge, UK

^v H. D. Flack (1983). *Acta Cryst A* 39: 876–881